ERDC/CHL TR-13-6

Coastal and Hydraulics Laboratory

US Army Corps
of Engineers®
Engineer Research and
Development Center

ERDC
INNOVATIVE SOLUTIONS
for a safer, better world

2D Hydrodynamic Investigation of Olmsted Cofferdams

Jeremy A. Sharp, Tate O. McAlpin, Ronald E. Heath,
Gary C. Lynch, and Howard E. Park

July 2013

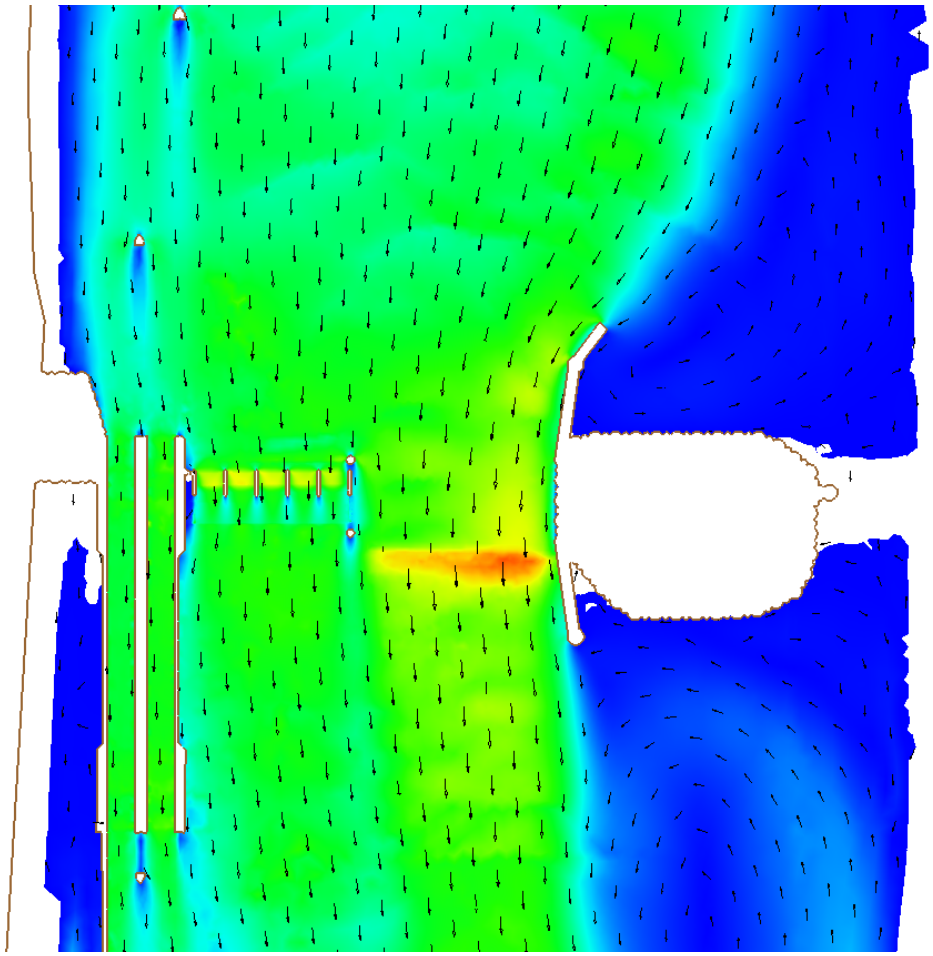

The US Army Engineer Research and Development Center (ERDC) solves the nation's toughest engineering and environmental challenges. ERDC develops innovative solutions in civil and military engineering, geospatial sciences, water resources, and environmental sciences for the Army, the Department of Defense, civilian agencies, and our nation's public good. Find out more at www.erdc.usace.army.mil.

To search for other technical reports published by ERDC, visit the ERDC online library at http://acwc.sdp.sirsi.net/client/default.

ERDC/CHL TR-13-6
July 2013

2D Hydrodynamic Investigation of Olmsted Cofferdams

Jeremy A. Sharp, Tate O. McAlpin, Ronald E. Heath, Gary C. Lynch, and Howard E. Park

Coastal and Hydraulics Laboratory
US Army Engineer Research and Development Center
3909 Halls Ferry Road
Vicksburg, MS 39180

Final report

Prepared for US Army Corps of Engineers Louisville District
Romano Mazzoli Federal Building
600 Dr. Martin Luther King, Jr. Place
Louisville, KY 40202

Abstract

The Olmsted Locks and Dam are currently being constructed on the Ohio River just downstream of Lock and Dam 53 at river mile 964.4. The original Olmsted construction plan called for an in-the-dry (ITD) construction using a four-phase cofferdam configuration; however, as a cost saving measure, planners changed the original plan to construct the dam using an in-the-wet (ITW) construction process. Cost and schedule concerns with ITW have US Army Corps of Engineers (USACE) leaders investigating all options to minimize overall project cost, time, and navigation impacts. Thus, USACE Louisville District (LRL) has proposed a two-phase cofferdam plan to replace the ITW construction. To evaluate the effect of the newly proposed cofferdam configurations the Adaptive Hydraulics Code (AdH) was applied to develop a model to provide current velocities and depths for the Ship Tow Simulator (STS) for pilots to evaluate the navigability of the proposed cofferdam configurations. In addition, AdH was used to evaluate areas of scour around the cofferdams qualitatively. Two stages and discharges were simulated. A maximum velocity through the navigation passes are from 10 – 18 feet per second (fps), and bed shear stresses are estimated at 14 -75 Pascals (PA). Both could negatively affect the viability of this two-phase cofferdam construction alternative.

Contents

Figures and Tables

Figures

Tables

Preface

The work was performed by the River Engineering Branch (HF-R) of the Storm Protection Division (HF), US Army Engineer Research and Development Center – Coastal and Hydraulics Laboratory (ERDC-CHL). At the time of publication, Dr. Loren L. Wehmeyer was Chief, HF-R; Dr. Ty V. Wamsley was Chief, HF; and Bill Curtis was the Technical Director for Flood and Storm. The Deputy Director of ERDC-CHL was Jose E. Sanchez and the Director was Dr. William Martin.

COL Kevin J. Wilson was the Commander of ERDC, and Dr. Jeffery P. Holland was the Director.

Unit Conversion Factors

Multiply	By	To Obtain
cubic feet	0.02831685	cubic meters
feet	0.3048	meters
knots	0.5144444	meters per second
miles (U.S. statute)	1,609.347	meters
pounds (force) per square foot	47.88026	pascals
yards	0.9144	meters

1 Introduction

The Olmsted Locks and Dam (L&D) have been through several construction design iterations. Recently the US Army Corps of Engineers (USACE) US Army Engineer Research and Development Center (ERDC) was requested to review the *Olmsted In-the-Dry H&H Agency Technical Review (ATR) Submittal Package,* dated 2 April 2012, prepared by the USACE, Louisville Engineer District (LRL). The LRL document references prior investigations. It was compiled to address further construction changes outside previously studied efforts. The LRL ATR document delivered a thorough analysis of potential impacts of the newly proposed two-stage cofferdam plan from previous studies. To further reduce uncertainties identified in the document and the ERDC review, the new construction plan required additional model investigations, which are documented in this report.

1.1 Background

The Olmsted Locks and Dam are currently being constructed on the Ohio River (see Figure 1) just downstream of Lock and Dam 53 at river mile 964.4. The new navigation locks and dam will replace the older upstream Locks and Dams 52 and 53. When complete, the structure will consist of three key features; two lock chambers 110-ft wide by 1200-ft long, five tainter gates each 110-ft wide, and a 1662-ft navigable pass section consisting of a 1400-ft-wide wicket gate section (see Figure 2). The locks will be operated during periods of low flow while the wicket gates are up. During high flow, the wicket gates will be lowered and navigation will proceed over the wicket gates.

Historically, dams have been constructed with cofferdams (also called in-the-dry (ITD) construction). Cofferdams create a hydraulic choke point in the river by blocking flow area, thus changing flow conditions. This includes, but is not limited to, changes in water surface elevations (WSE), velocities, unit discharge, bed transport potential, and bed shear stress. Increased velocities in a navigation channel are potentially hazardous for both the structure (due to the potential for scour undermining the structure) and navigational maneuvering.

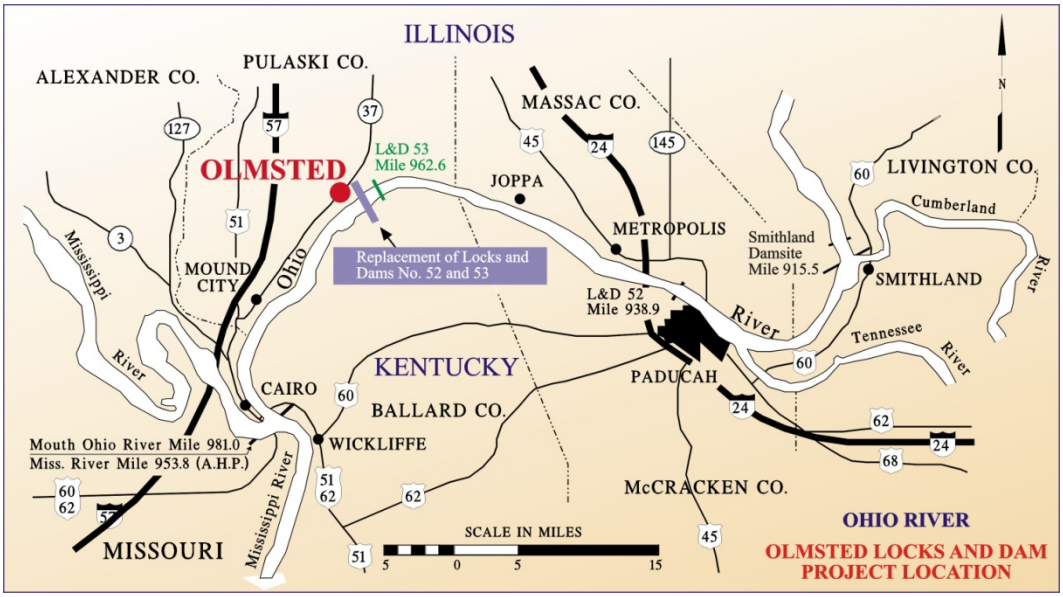

Figure 1. Olmsted Locks and Dam project location.

The original Olmsted construction plan called for an ITD construction using a four stage cofferdam configuration; however, as a cost saving measure, planners changed the original plan to construct the dam using an in-the-wet (ITW) construction process and eliminate the need for three of the cofferdam structures. The ITW process requires the use of SCUBA divers, but persistent adverse flow conditions have limited the time that SCUBA divers can safely work. This factor, combined with other cost and schedule concerns, have USACE leaders investigating all options to minimize overall project cost, time, and navigation impacts.

In place of the original cofferdam configurations, LRL has developed an alternate construction methodology to complete the navigation pass section of the dam by means of a two-stage cofferdam configuration. The original four-stage cofferdam configuration required modification, since both the lock chambers and the tainter gate sills are or will already be in place. The locks were constructed using the original cofferdam layout while the tainter gates are presently being placed using ITW construction.

For the new configuration, the first stage cofferdam (Phase 1) is located on the Kentucky side of the river and allows 790-ft of open river navigation between the tainter gates and cofferdam. The second stage cofferdam (Phase 2) is adjacent to the tainter gates and allows 700-ft of navigation over the newly constructed wicket gate section (navigation pass) from Phase 1 on the Kentucky side.

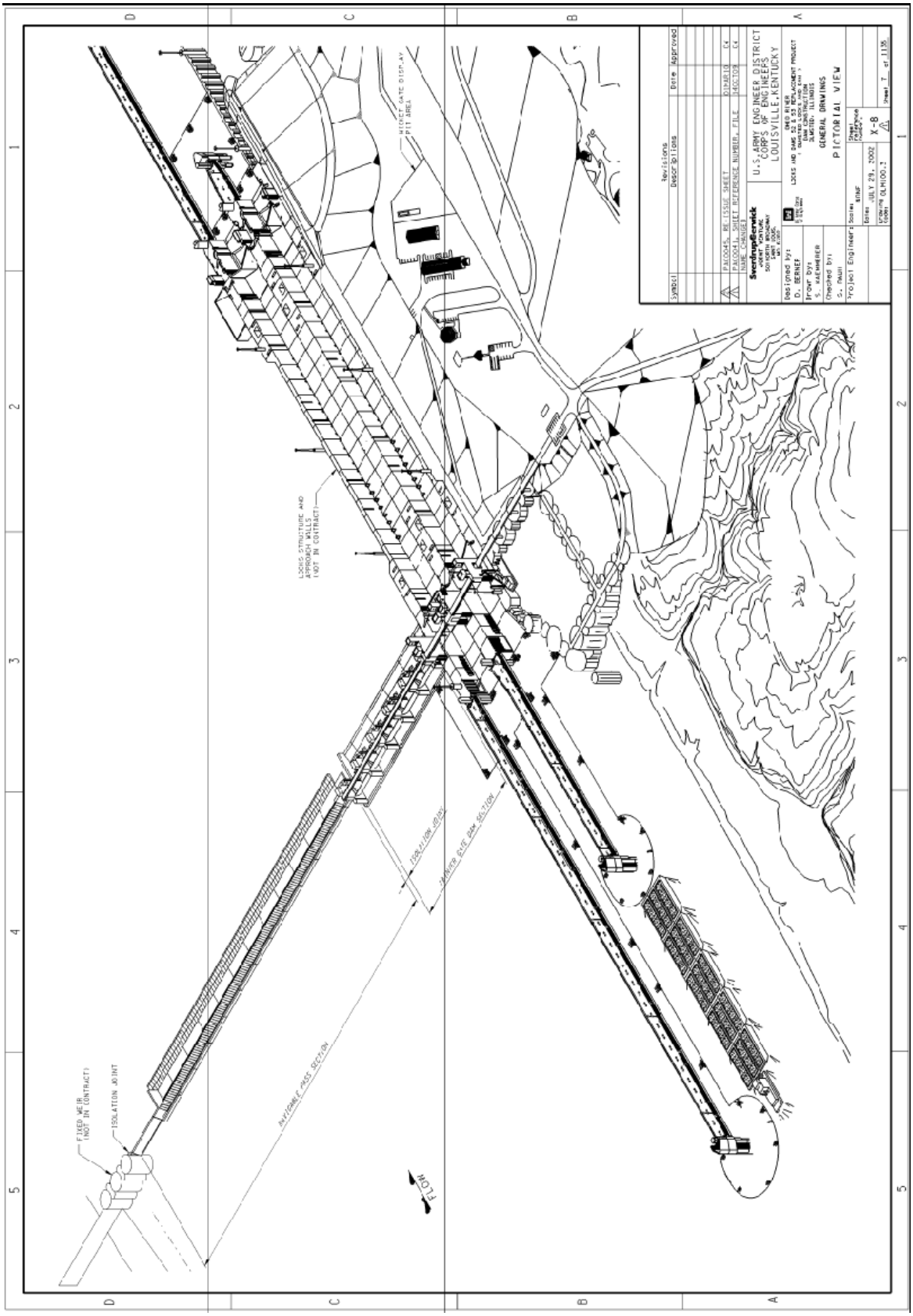

Figure 2. Olmsted Locks and Dam construction plan schematic.

1.2 Study history

Both physical and numerical modeling has been conducted for the Olmsted Locks and Dam project. Early efforts used physical models to evaluate scour and navigation issues, with numerical models implemented later. The US Geological Survey (USGS) used RMA-Z (Wagner 2004) to predict effects of the ITW phased construction and operation on mussel beds located downstream (RMA-Z 2004). Then in 2008, CHL used an Adaptive Hydraulics model (AdH) to further evaluate potential impacts on mussel beds. In 2012, LRL used a HEC-RAS model to estimate impacts (maximum velocities through the passes and swell-head) from the new cofferdam concept.

Original study efforts began in 1987 as the basis for ITD construction. For the ITD study, the predecessor to ERDC, the USACE Waterways Experiment Station (WES), used a 1:120 scale fixed-bed physical model. The model extended from Ohio River Mile (RM) 965.9 to (RM) 962.5. Multiple dam designs were evaluated to determine the ideal configuration. This included various widths of wicket gates and various numbers of tainter gates. Designers decided to go with an all wicket gate structure that was 2200-ft wide. Tests evaluated navigation conditions for various cofferdam configurations over a range of flow conditions for the all wicket gate design. From these tests, it was decided to use a four-stage cofferdam configuration. Construction would begin on the Illinois side with the locks and work to the Kentucky bank.

Additional testing was later done (2005 – 2008) to evaluate whether ITW construction was feasible. This effort was performed with the same 1:120 scale model (PM 1997) of the original study along with a 1:60 scale model. Additional efforts included evaluating different dam configurations and cofferdam layouts. A three stage cofferdam configuration was recommended. From this effort the original design was modified to six tainter gates, 1300-ft of navigable wicket gates, and floating approach walls. The recommendation for construction was heavy lift-in ITW construction techniques. The number of tainter gates was later reduced to five and the navigation pass width increased to 1400 ft.

Numerical model investigations were conducted after the physical studies by the USGS and the ERDC. One of the first of these was the USGS RMA-2 model (RMA-2 2004). This model evaluated the effects of the phased construction and operation. Both a hydraulic model and sediment model

were created. This model extends from RM 974.5 to 962.6 allowing inclusion of downstream mussel beds. In the USGS study, hydrodynamics, sediment transport, and mussel bed impacts were evaluated.

An additional evaluation of the mussel beds was performed in 2008 by the ERDC using AdH 2008. The AdH covered the same domain as RMA 2004 and used the same properties and boundary conditions. Data from these numerical models were utilized for the current modeling effort to determine the navigability and scour potential of the newly proposed construction process.

2 Modeling Approach

To evaluate the effect of the newly proposed cofferdam configurations, the AdH model was developed to provide velocities and depths for the Ship Tow Simulator (STS) in order for pilots to evaluate the navigability of the proposed cofferdam configurations. In addition, AdH was used to qualitatively evaluate areas of scour around the cofferdams.

Three AdH meshes were constructed. The first represents the Phase 1 Cofferdam configuration, the second represents the Phase 2 Cofferdam configuration, and the third represents the final dam configuration. Due to time constraints, the modeling effort was expedited by not developing an existing condition mesh. Typically, the existing condition run is used for model validation. However, prior knowledge from the RMA 2004 and AdH 2008 models was applied here. This does not imply that the new model is validated or replicates the old models; rather, the participating engineers believe that, given the time constraints, it is sufficient for the purpose of this study.

Details from both RMA 2004 and AdH 2008 were implemented for the present AdH application (AdH 2012). From the USGS model, overbank topography and some structural bathymetry (wicket gates section, tainter gates and tainter spillway) were updated. The upstream flow distribution from the USGS model was applied. Details used from the AdH 2008 included mussel bed mapping and surface roughness (Manning's values). Other items such as horizontal projection and channel alignment were corrected from the AdH 2008 to ensure proper placement of key features.

3 Model Development

3.1 Boundary conditions

Two steady-state flow conditions were requested by LRL to analyze navigation and bed shear of both cofferdam phases. Condition 1 is a discharge of 300,000 cfs and a WSE at the structure of 295 ft (Ohio River Datum). Condition 2 is a discharge of 951,000 cfs and a WSE at the structure of 320 ft (Ohio River Datum). Both of these flow conditions represent high velocity scenarios. A series of runs were necessary to determine the appropriate downstream boundary for each condition that resulted in the desired WSE. For Condition 1, the downstream boundary was 290.1 ft (Ohio River Datum) and for Condition 2, it was 315.4 ft.

The control at the upstream end of the model domain is Locks and Dam (L&D) 53. Flow distribution at the upstream boundary is a key component to the modeling effort and is complicated by the configuration of L&D 53. L&D 53 has a 932 ft navigation pass comprised of wicket gates, a 340 ft Chanoine weir, a 160 ft Bebout weir, two 90 ft beartraps, a 102 ft fixed weir, and a 1778 ft core wall. These structures have sill elevations that range from 270 – 280 ft (Ohio River Datum). To capture the flow distribution downstream of L&D 53, the USGS conducted a series of surveys in the late 1990s (Wagner 2004). Measurements were collected for three different flow conditions: 72,500; 350,000; and 770,000 cfs at WSE of 288.3, 307.2, and 323.5 ft (Ohio River Datum), respectively. From these data, the flow distribution for the boundary conditions were derived and adapted here (see Table 1 for the flow distribution and Figure 3 for the location of the boundary strings).

Table 1. Flow distribution in AdH 2008 and AdH 2012 based on Wagner (2004).

	Flow Distribution	
	Condition 1	Condition 2
Discharge, cfs	300,000	951,000
Left String	25%	25%
Middle String	18%	22%
Right String	57%	53%

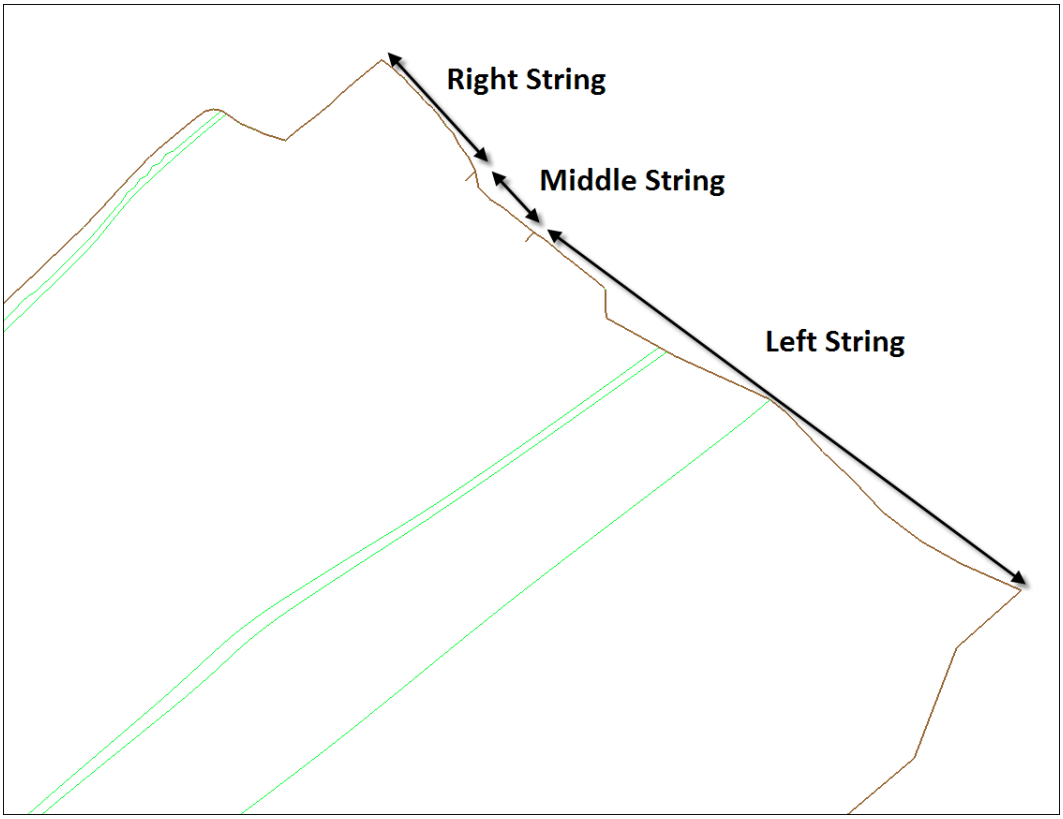

Figure 3. Location of upstream discharge boundary strings for AdH 2008 and AdH 2012.

For model initiation, hot start files were generated using a constant water surface elevation, typically the tailwater elevation boundary condition. These initial depth conditions were allowed to spin up, reaching steady-state over two days. The AdH was used in its dynamic form and not in the steady-state option. This allowed for complex temporal and spatially varying shedding vortices to form, and was done so that adverse currents could be detected in the model. Flux lines were used as the primary check on the convergence to steady-state. The flux lines near the upstream and downstream boundaries represented the total incoming and outgoing discharge. The simulations were at steady-state when the difference in discharges at the flux lines converged to zero (see Figures 4 and 5). Three of the four simulations converged to zero as expected.

However, the Phase 2 Condition 1 (see top of Figure 5) showed perturbations of flow at the flux lines. These perturbations were approximately 50 cfs different, representing 0.017 percent of the total flow, and were shown to be a direct result of the vortex shedding that occurred downstream of the Phase 2 cofferdam.

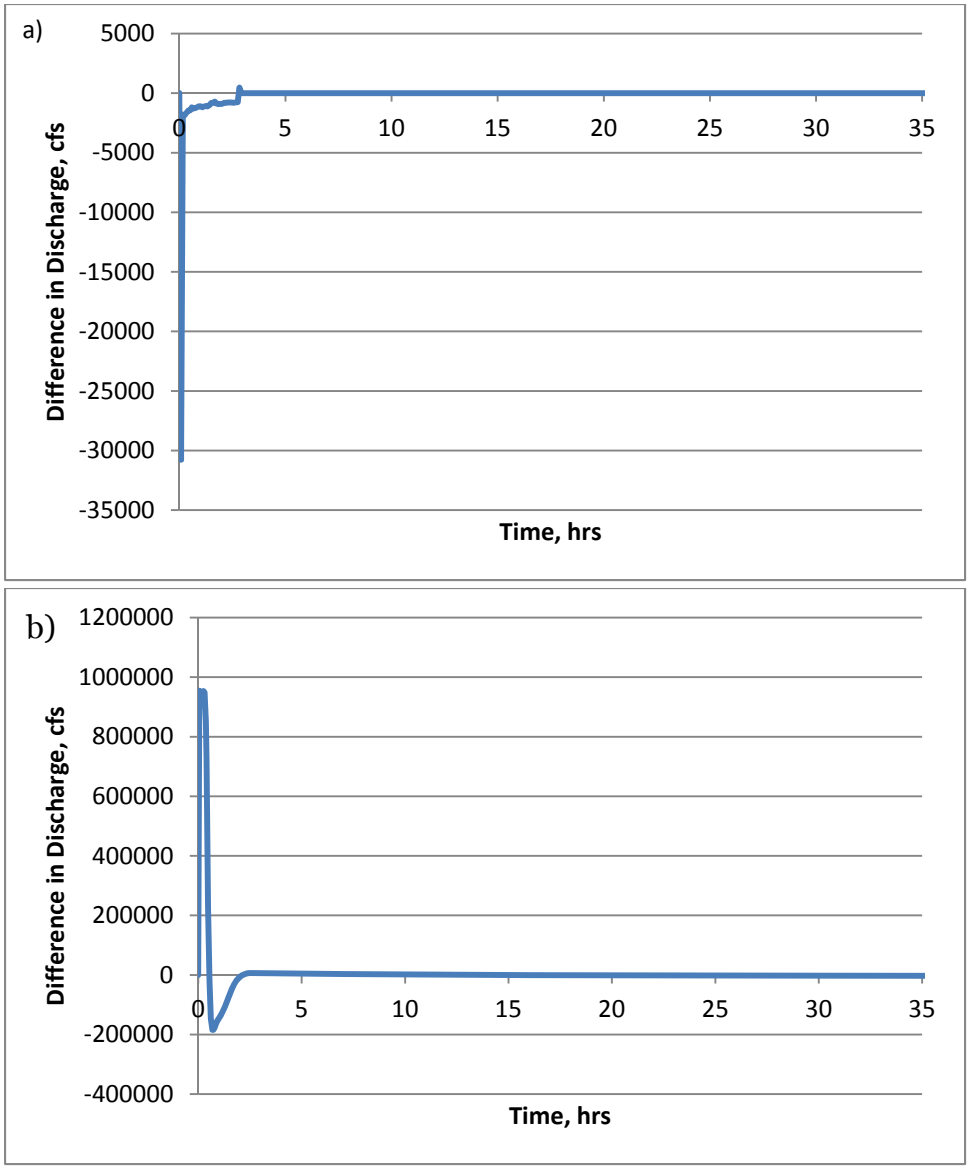

Figure 4. Steady-state check for a) Phase 1 - Condition 1 and b) Condition 2.

3.2 Meshes

With the exception of a portion of the structures, the RMA 2004 and AdH 2008 models were the starting points for the AdH 2012. Once adjusted and re-projected, the AdH 2008 was converted to a map file in the Surface Water Modeling System (SMS). The SMS is a pre- and post-processor used to aid mesh generation and data visualization. The map file was then overlaid with a shape file of the structures (see Figure 6). The shape file was used to locate emergent features of the structure, such as lock walls, guide walls, guard walls, tainter gate piers, and cells. These features were mapped in SMS along with the cofferdams for both Phase 1 and 2, and the final dam

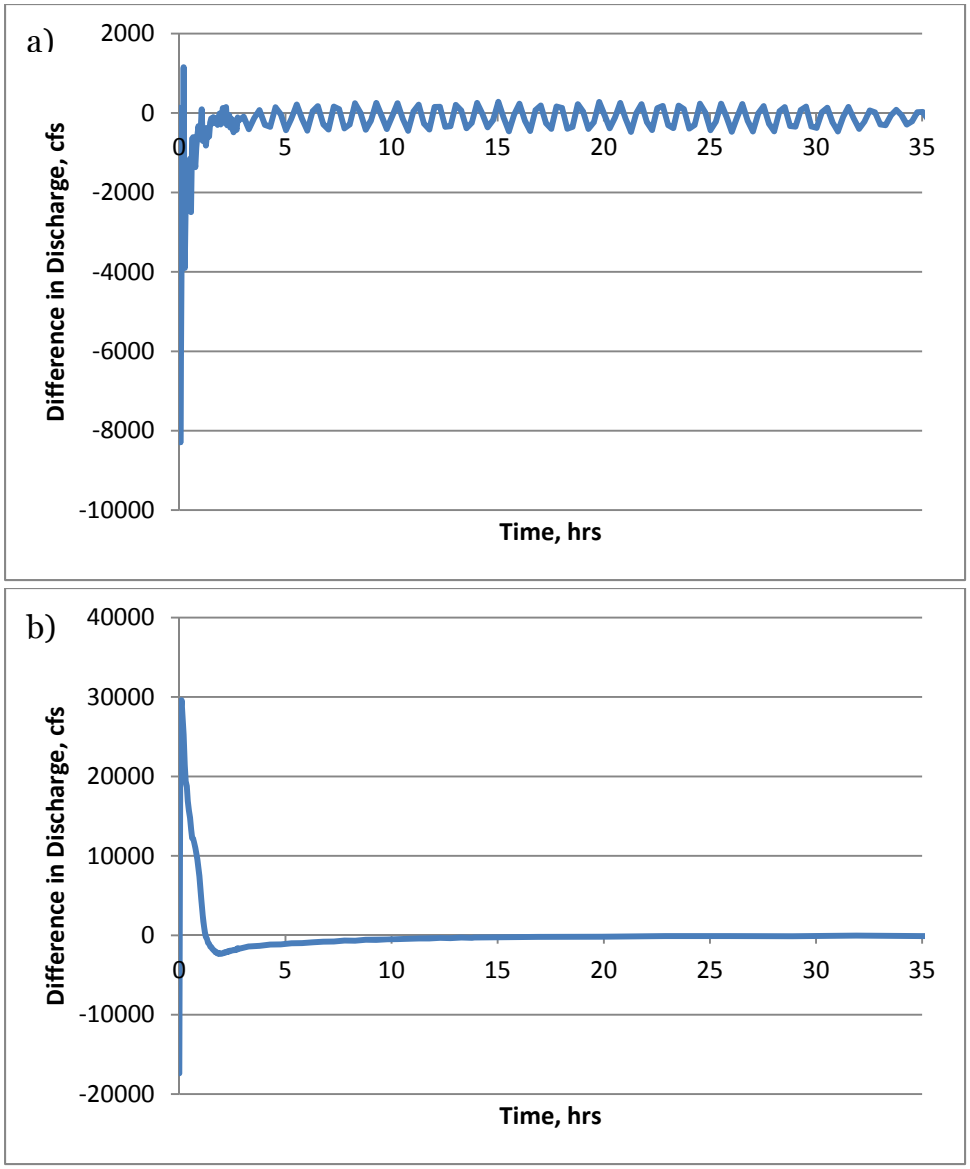

Figure 5. Steady-state check for a) Phase 2 - Condition 1 and b) Condition 2.

configuration. From the map files, the meshes were generated in SMS. The Phase 1 mesh (see Figures 7 and 8) has 76,156 nodes and 149,967 elements. The Phase 2 mesh (see Figures 7 and 9) has 77,369 nodes and 152,277 elements. The final dam configuration mesh (see Figure 10) has 73,425 nodes and 145,083 elements. The mesh's channel element size ranged from 10 – 25 ft. The elements through the tainter gates were 2 -8 ft. The element size in the locks was 15 – 25 ft. The element size in the overbank areas was 100 – 1000 ft.

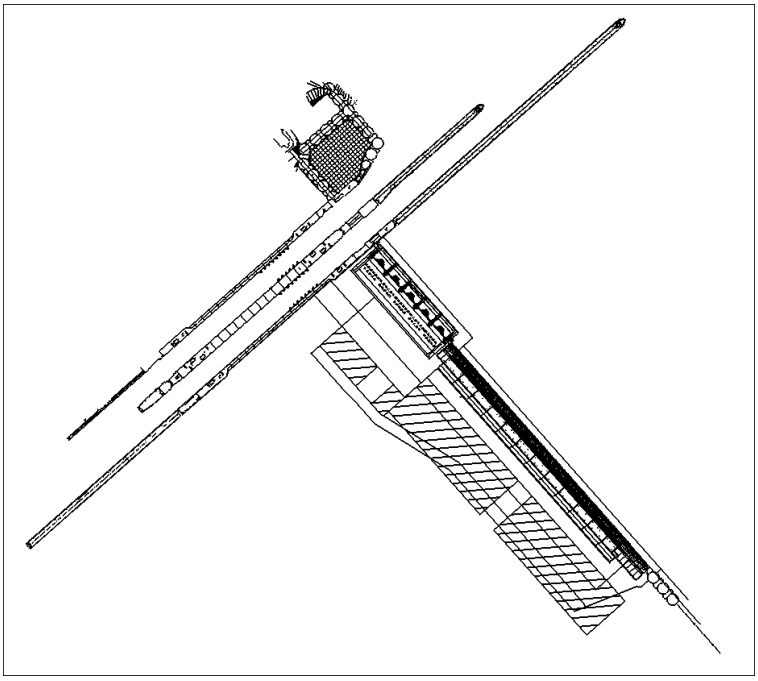

Figure 6. Shape file of the Olmsted Locks and Dam structures.

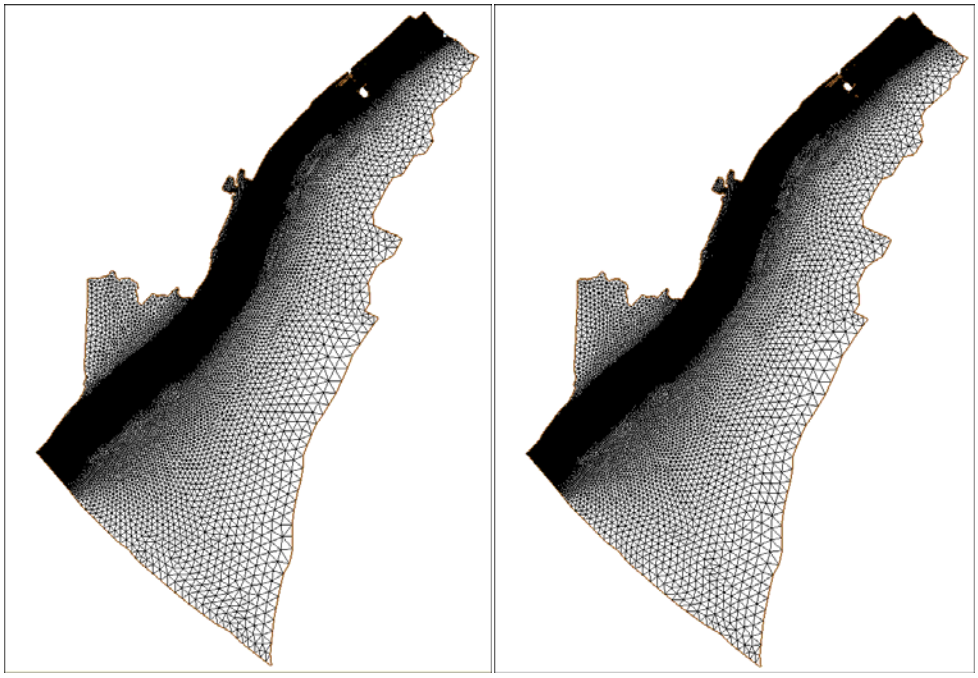

Figure 7. Domain extents for Phase 1 (left) and Phase 2 (right).

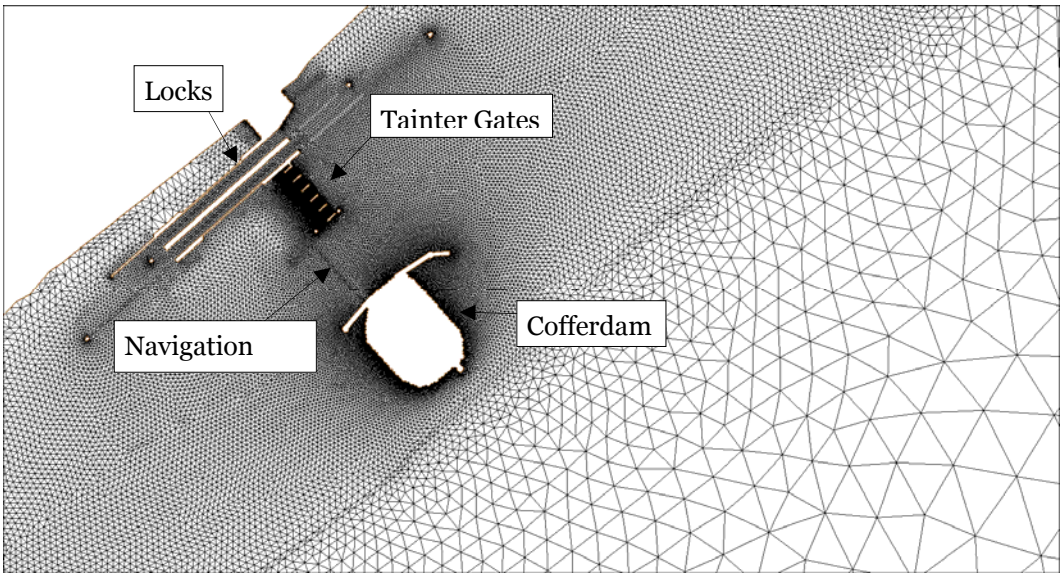

Figure 8. Phase 1 locks, tainter gates, navigation pass, and cofferdam placement in mesh.

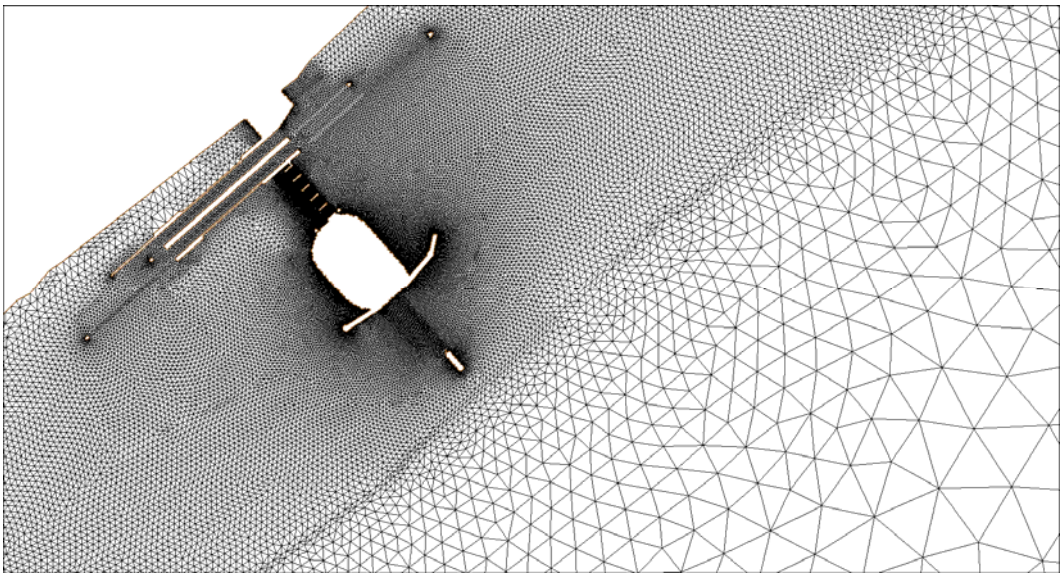

Figure 9. Phase 2 locks, tainter gates, cofferdam, and navigation pass placement in mesh.

For the AdH 2012, the domain extended from RM 974.5 to RM 962.6 and includes the mussel beds downstream of the site as well as the downstream side of L&D 53. The domain bounds were based on previous studies. All horizontal data were re-projected to Kentucky State Plane South, zone 1602, NAD29 (ft), and vertical data of Ohio River Datum (ft).

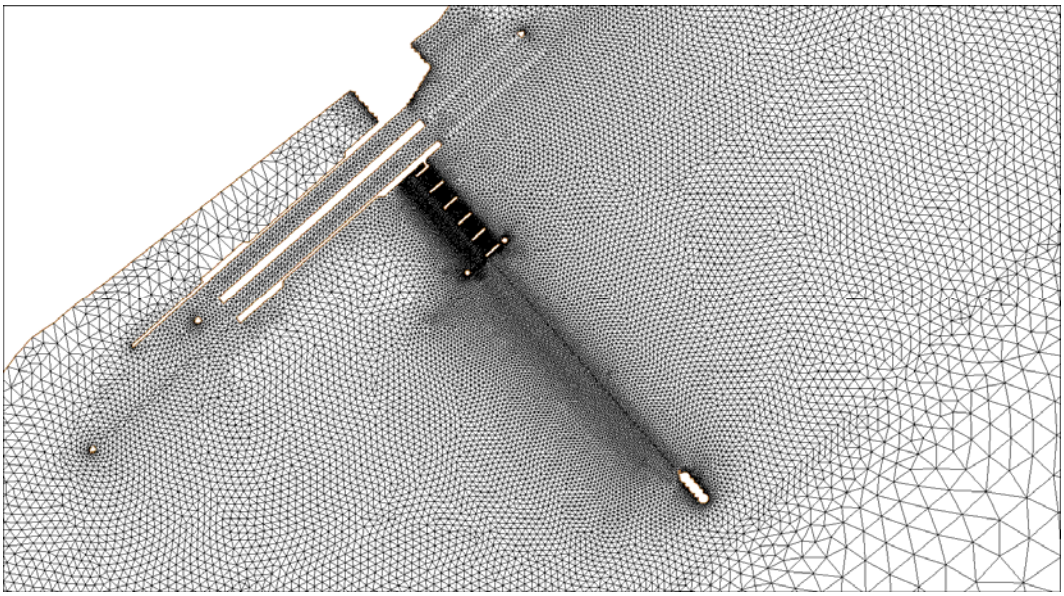

Figure 10. Final dam configuration mesh.

The LRL provided the August 2011 Olmsted Locks & Dam Construction Annual Mussel Monitoring Survey, which included bathymetry from RM 962 to RM 970. These files were merged and filtered in SMS using a filter angle of five deg, which reduces points whose tangential angle is less than five deg. This filtered dataset captured the bathymetry and reduced the files to a more manageable size. Beyond the extents of the annual survey, bathymetry from the AdH 2008 was applied, primarily in the overbank areas and downstream of RM 970. For bathymetry in the construction area (this is the bathymetry that has the largest impact on local flow conditions) , a 2.0 ft resolution survey from May 2012 that extended from RM 964.7 to RM 964.1 was filtered and merged into the combined dataset of the annual survey and previous model study bathymetries. The three merged bathymetry datasets were mapped onto the meshes (see Figures 11– 13).

Materials are assigned in the model to define the skin friction via Manning's value (see Table 2) and the eddy viscosity. Spatially, the meshes used the same materials. The only differences exist in Phase 2 and the final dam configuration where a material was added for the wicket gate section. Material locations are shown in Figures 14 and 15.

3.3 Pressure field simulations

In reality, there are real-time vessel/current interactions where near and far field currents are impacted directly by a moving vessel. This is especially true in locations where there is a structure or tight channel. Unfortunately,

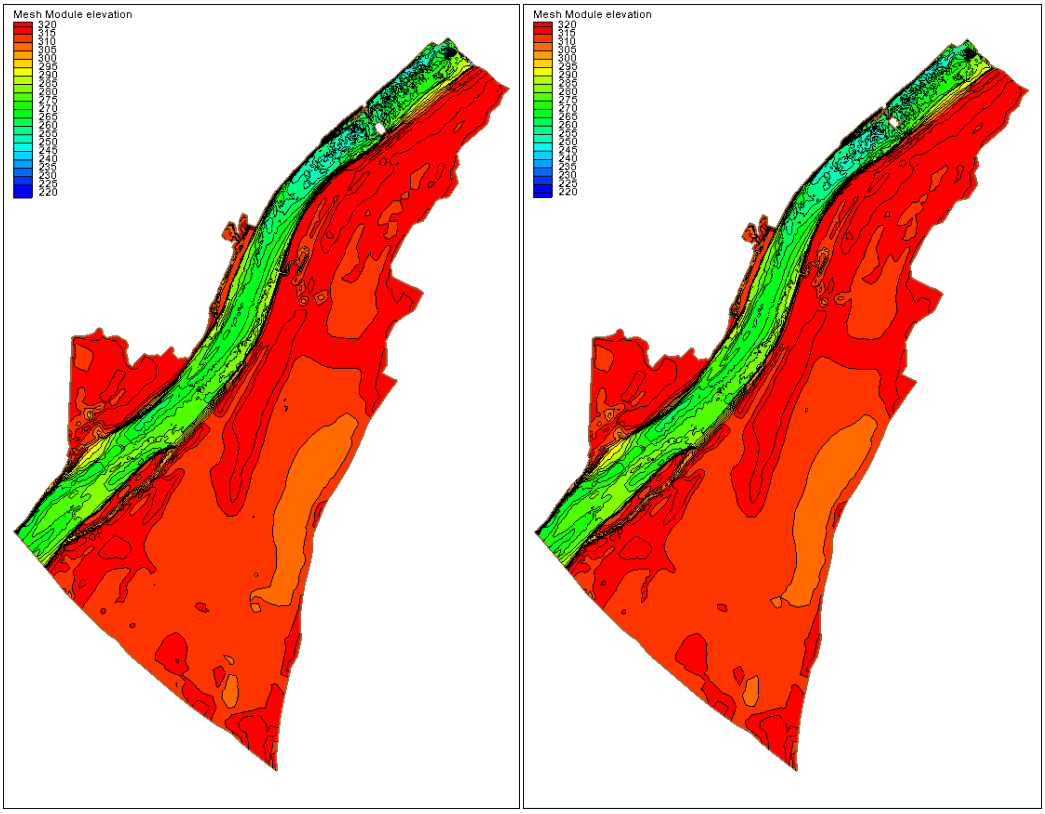

Figure 11. Site elevations above the Ohio River Datum for Phase 1 (left) and Phase 2 (right).

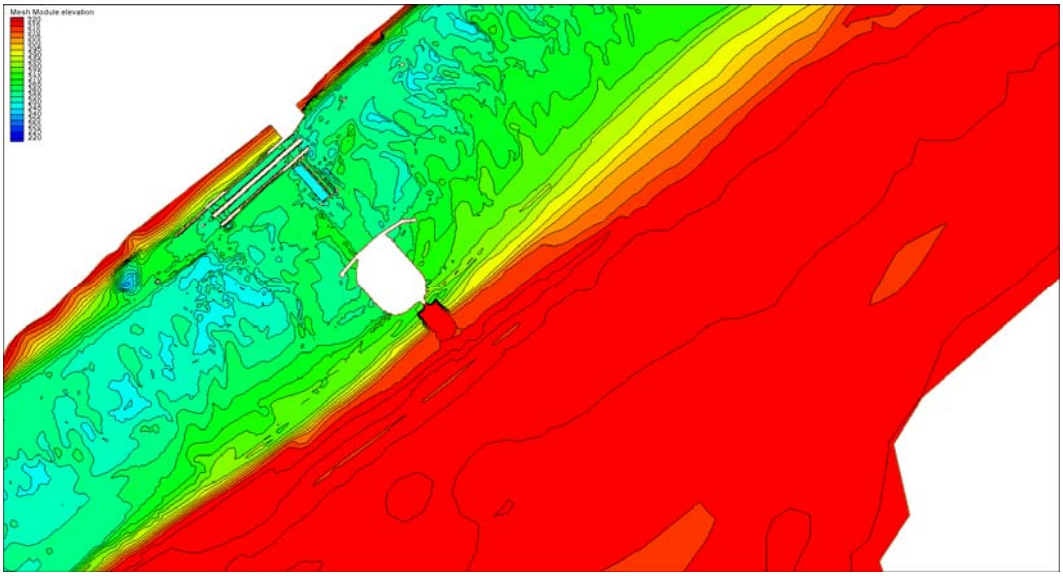

Figure 12. Phase 1 site elevations above the Ohio River Datum in mesh.

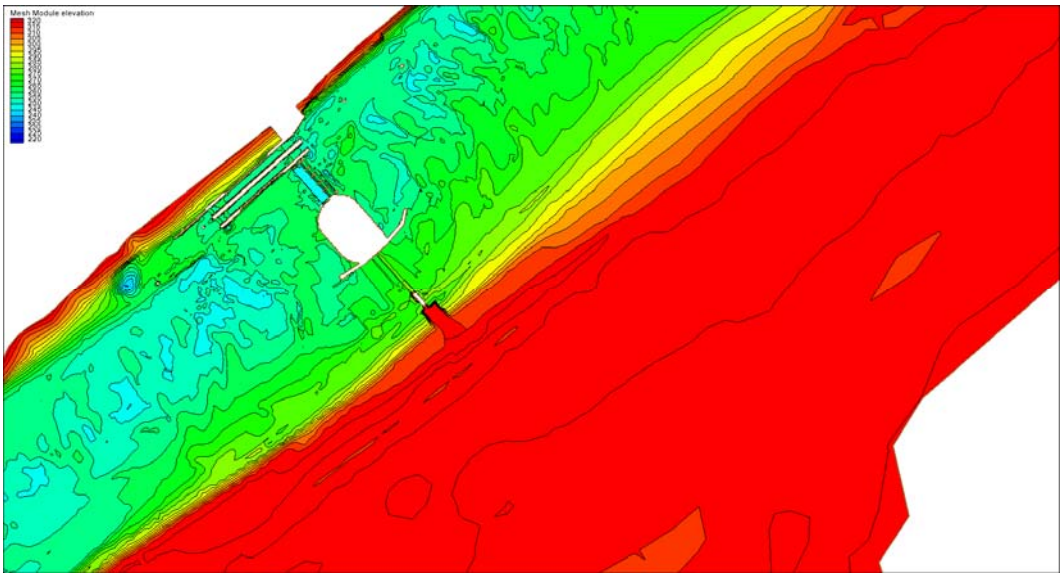

Figure 13. Phase 2 site elevations above the Ohio River Datum in mesh.

Table 2. Model materials.

Material Number	Material Name	Manning's Value
1	Channel	0.02 - 0.03
2	Bank	0.045
3	Overbank	0.045
4	Innerbank	0.036
5	Lower mussel bed	0.025
6	Outer mussel bed	0.025
7	Inner mussel bed	0.025
8	Rock dike	0.04
9	Rip-rap upstream	0.035
10	Rip-rap middle	0.04
11	Rip-rap downstream	0.035
12	Lock chambers	0.015
13	Ogee crest	0.015
14	Stilling basin	0.015
15	Baffle blocks	0.03
16	Guard walls	0.03
17	Outlet structure	0.015
18	Straight walls	0.015
19	Wicket gates	0.018

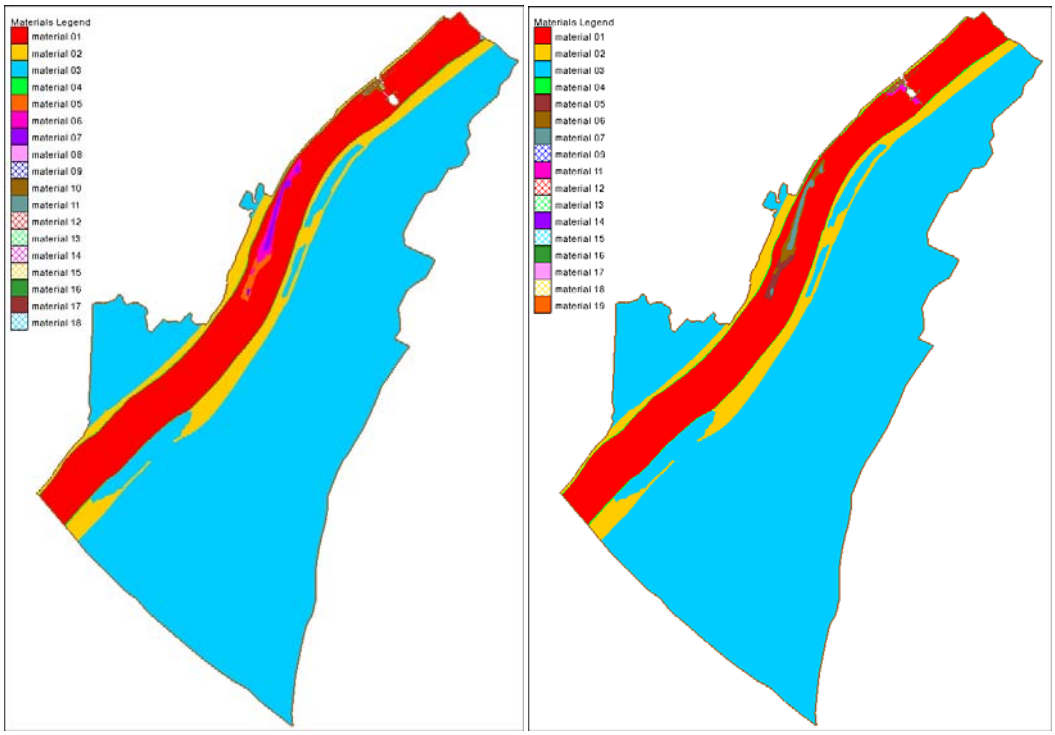

Figure 14. Material boundaries for Phase 1 (left) and Phase 2 (right).

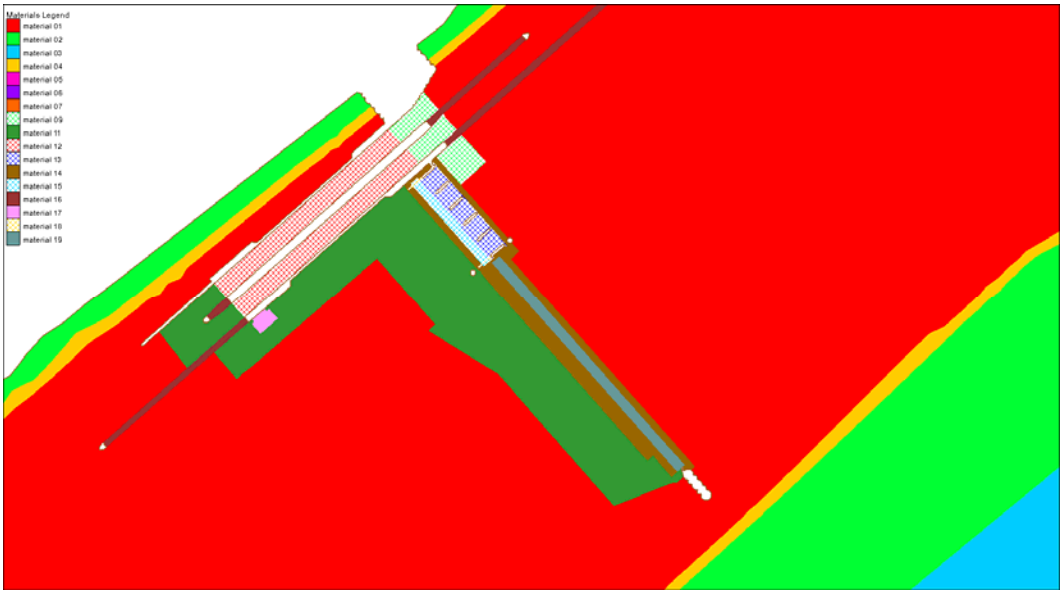

Figure 15. Final dam configuration materials.

this is beyond the current version of AdH's numerical modeling capability in the STS; however, it still requires consideration and some form of representation. Thus, a methodology was adapted that attempted to mimic impacts of vessel passage on the current field, thereby supplying the STS with a current field more representative of the natural environment.

A series of three boat paths were simulated for each phase and flow condition. The boat simulations used moving pressure fields in AdH to represent the movement of the design vessel (3x5 tow). These pressure fields do not represent prop-wash, or vertical accelerations associated with vessel movement. However, the pressure fields do displace the vessel "footprint" creating a drawdown and return current pattern (Berger and Lee 2005).

To match the vessel footprint, special considerations were required. Depths at nodes inside the area of the vessel were displaced to the proper draft using a pressure penalty term. The nodes on the edge of the vessel apply a linear interpolation to those under the vessel, sloping the sides of the vessel. These sloped sides change the desired blockage area. The blockage area of the vessel is important to match the peak drawdown (Stockstill and Berger 1999). The mesh adaption feature in AdH was utilized to represent the blockage of the vessel.

Five simulations with incremental increases in adaption were conducted to determine the necessary level of refinement. The shallow-water refinement tolerance (SRT) triggers the mesh refinement with a value of one for all levels of refinement/adaption. For a further discussion on SRT and AdH, see Berger and Stockstill (1999) or Stockstill and Berger (2001), and for selecting SRT values, see Berger and Lee (2005). The ERDC's main concern was the increases in velocity as a result of the vessel passage. Near field velocities increase through the pass due to the dynamic of vessel passage creating greater velocities than those without the vessel passage. The increased velocity due to vessel passage represents the velocities that must be overcome by the vessel. Thus, the peak velocity as the bow of the vessel crossed a cross-section in the navigation pass was evaluated for each level of refinement, 2 – 10 levels of refinement in increments of 2.0. It was determined that at four levels of refinement, the velocities stopped changing and final results could be reasonably obtained.

Four cross sections along with three boat paths defined the impacts of the pressure fields on the velocities for Phases 1 and 2. The change in velocity was captured at the twelve intersecting points of the cross-sections and boat paths (see Figures 16 and 17). The values were used to interpolate spatially the impact at all locations in the navigation pass. This limited the number of pressure field runs to six, while allowing representation of increased velocities at all locations throughout the pass.

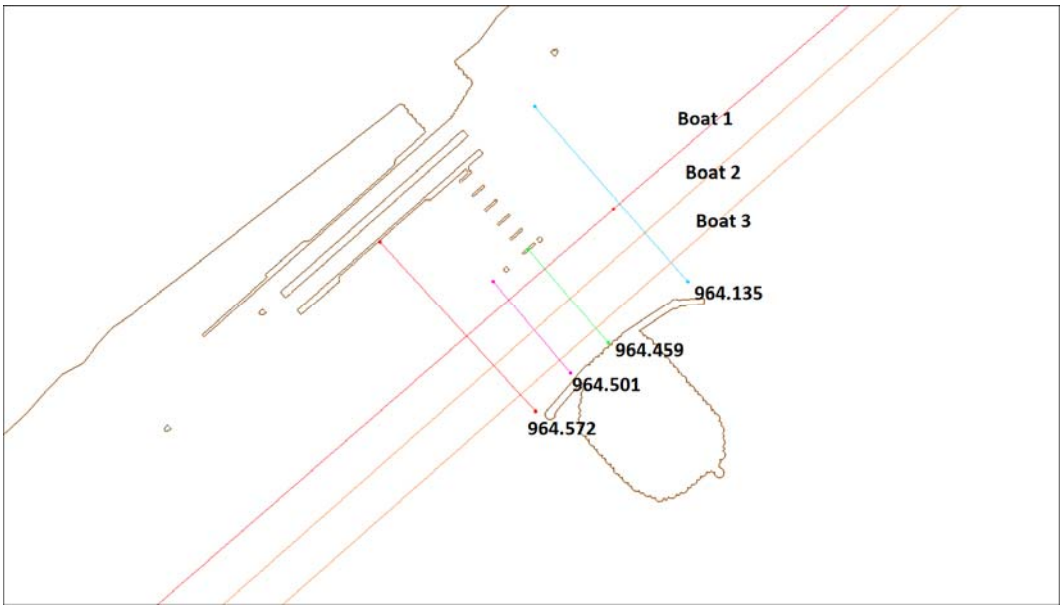

Figure 16. Cross sections and boat locations for Phase 1.

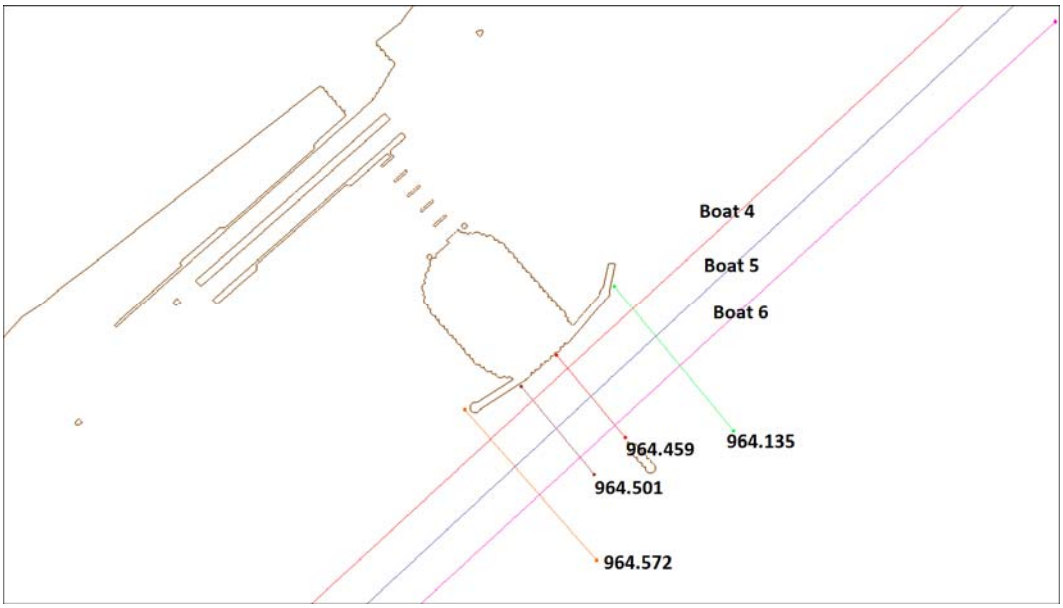

Figure 17. Cross section and boat locations for Phase 2.

4 Model Validation

To expedite the modeling process, a traditional existing conditions validation was not performed. Thus, alternative validation measures were required. This included comparing historic water surface slopes to structure in-place modeled water surface slopes. Then, a comparison of vortex shedding for an analytical solution and model solution was performed. Additionally, model comparisons were made between AdH 2012 and the LRL HEC-RAS model, RMA 2004, and PM 1997 for both velocities and water surface elevations.

4.1 Water surface slopes

The model water surface slopes were compared with the water surface slope between the Olmsted and Cairo gauges. From this comparison, the modeled water surface slope was shown to be reasonable, falling within the range of historic slopes (see Figure 18). The large variation in slope at a given WSE is the product of the influence of the Mississippi River. The Mississippi River is the tailwater control for the lower Ohio River.

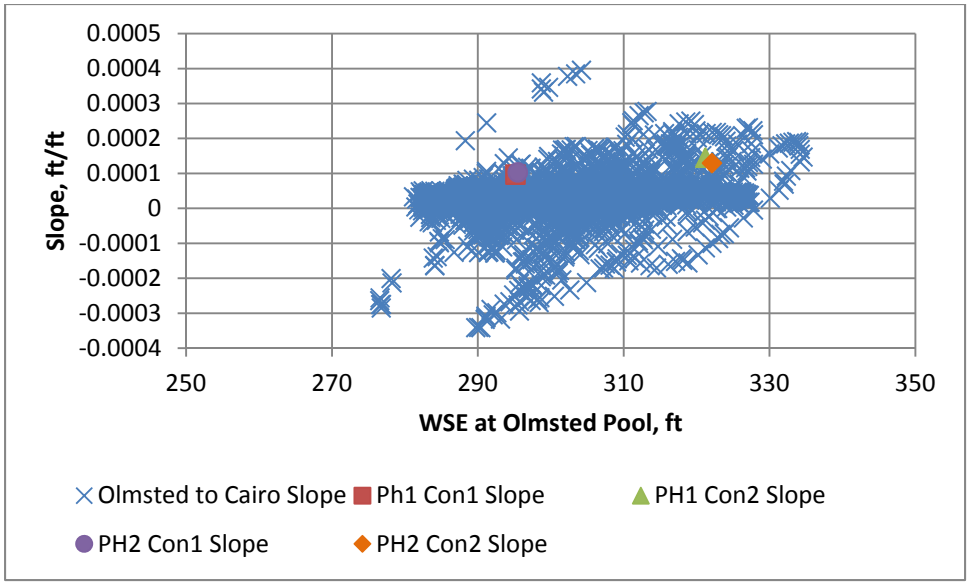

Figure 18. Slope comparison, Cairo to Olmsted.

4.2 Vortex shedding Phase 2

For Phase 2, the AdH 2012 simulates an oscillating flow condition downstream of the cofferdam. This is a classic example of vortex shedding

around a cylinder. The cofferdam in the middle of the flow field creates a separation of the streamlines. Any immersed blunt bodies where the Reynolds number (*RE*) is adequately large ($10^2 < RE > 10^7$) will create periodic shedding of vortices (Ahlborn et al. 2002). This shedding is called the von Karman vortex street, after T. von Karman who described the theory in 1912 for flow around cylinders (White 2003). The oscillating flow condition is typically defined as a function of both the Strouhal number (*ST*) and the Reynolds number (*RE*).

$$ST = \frac{fd}{U} \tag{1}$$

$$RE = \frac{\rho Ud}{\mu} \tag{2}$$

where

f = the frequency of vortex shedding,
d = the diameter of the cylinder,
U = the free stream velocity,
ρ = mass density, and
μ = the absolute viscosity.

AdH 2012 produced an oscillation period of 8.6 and 5.5 min (see Figure 19) for Conditions 1 and 2, respectively. These periods produce a *ST* of 0.28. For high *RE*s, the *ST* range can vary from the average of 0.21 to 0.31 (Jones 1968; Roshko 1961). These calculated values were deemed reasonable for the effort, and provided an additional measure of confidence. A time series of plots in Figures 20 and 21 represent a typical vortex shedding period.

4.3 Model comparison

Several model studies have been conducted for the Olmsted project over the years and provide an opportunity for model comparisons. While not ideal, a model comparison provides some assurance of model consistency. Here both LRL's new HEC-RAS model and PM 1997 were used for the Olmsted Locks and Dam old and new ITD hydrodynamic conditions comparison (see Tables 3 – 6).

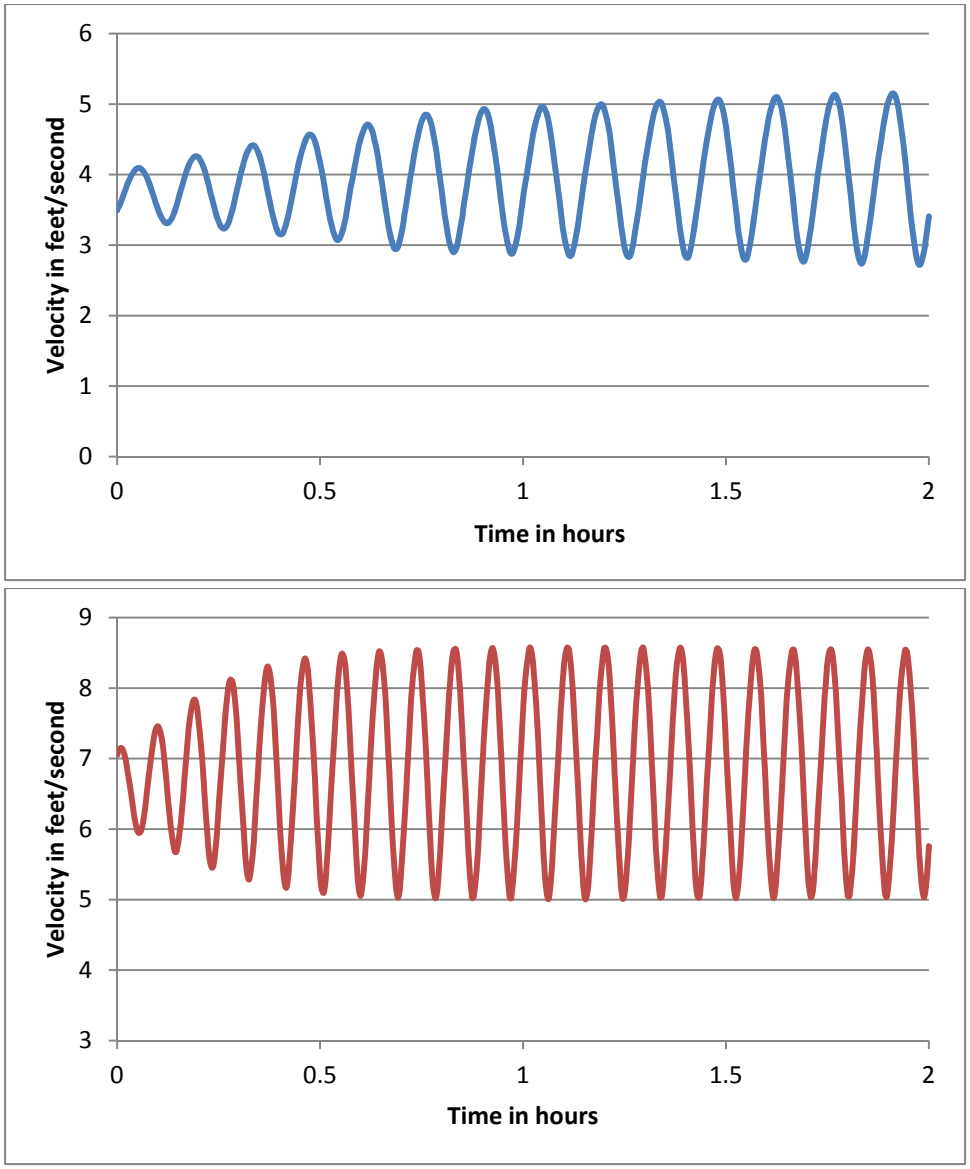

Figure 19. Vortex oscillation for Conditions 1 (top) and 2 (bottom) at a point downstream of the cofferdam.

These comparisons were originally done by LRL between the PM 1997 and HEC-RAS models. The comparisons were used as a calibration for HEC-RAS since the PM 1997 had been validated to field data. Note that the PM 1997 model was for a different cofferdam configuration while HEC-RAS simulated the new configuration.

For comparisons to be conducted between the original cofferdam configuration and the proposed configuration, similarities between the two were evaluated. The conditions that most closely resembled each other were compared. This included comparing the Stage A cofferdam from PM 1997

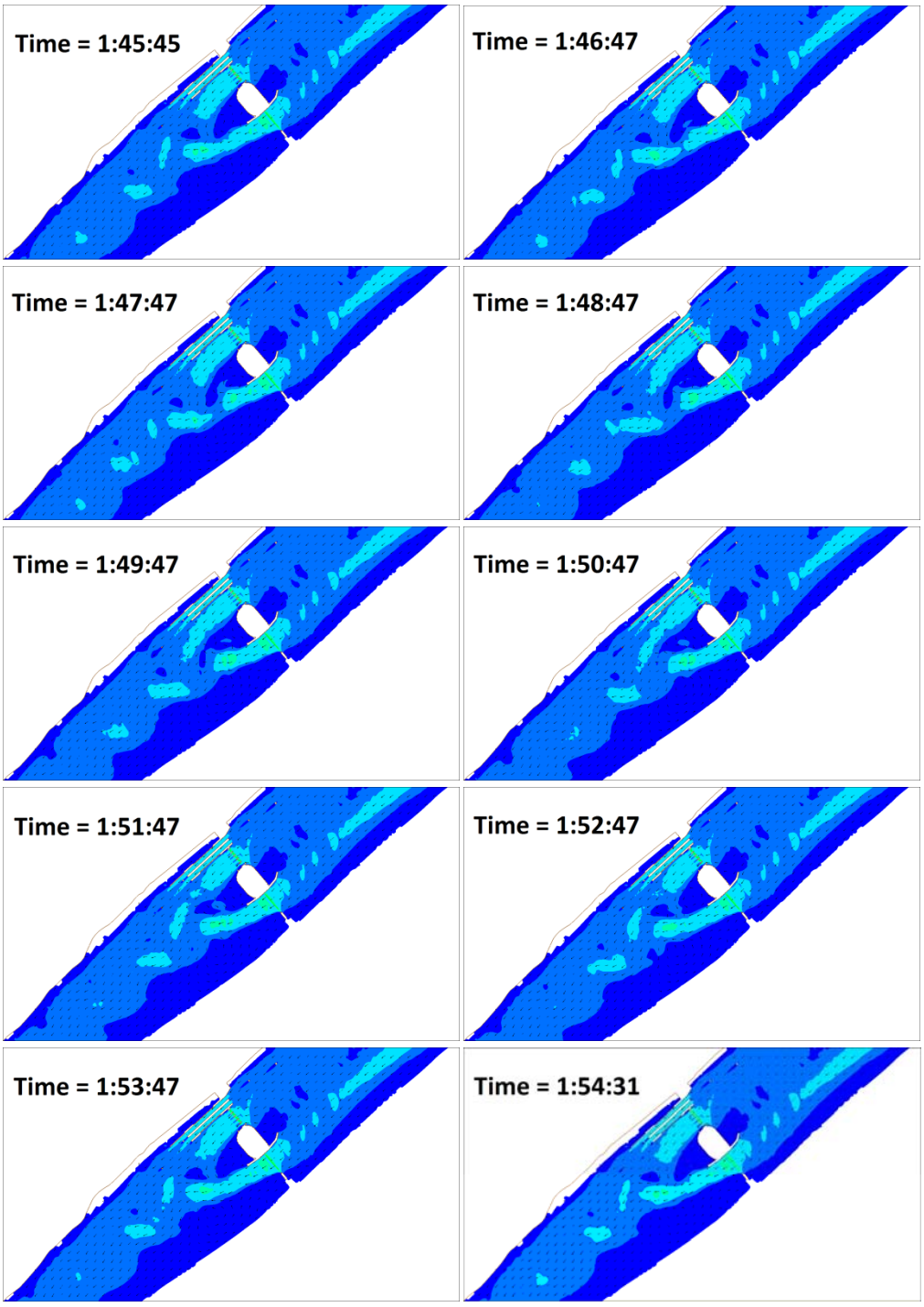

Figure 20. Time series of velocity contours showing eddy formation downstream for Condition 1.

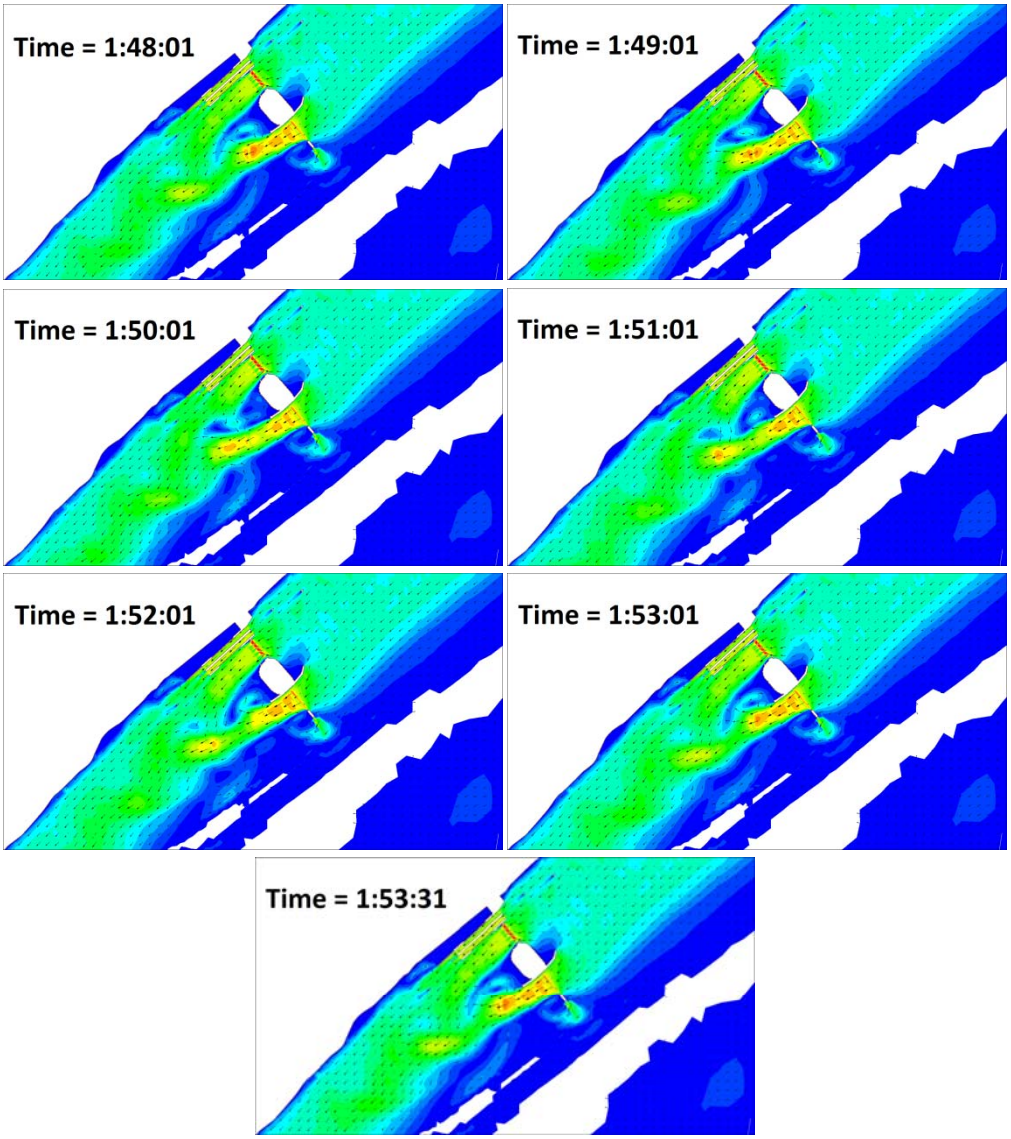

Figure 21. Time series of velocity contours showing eddy formation downstream for Condition 2.

(from the original configuration) to the Phase 1 Cofferdam from HEC-RAS and AdH 2012. Then the Stage B Cofferdam from PM 1997 was compared to the Phase 2 Cofferdam from HEC-RAS and AdH 2012. For the Phase 1 Cofferdam, the total river pass width is 1560 ft and 920 ft for Stage A. Although they differ on river pass widths, the main reasoning for the association is the location of both cofferdams on the Kentucky bank side. Both allow limited diversion from the main thalweg of the channel. For the Phase 2 Cofferdam, the total river width is 1470 ft while Stage B is 1560 ft. Phase 2 and Stage B are aligned in the center of the channel and block off a portion of the thalweg of the river.

Table 3. Water surface elevations (Ohio River Datum in ft) and swell head comparisons for Phase 1.

	Phase 1 - Condition 1		
X-Sec (RM)	HEC-RAS	AdH 2012	PM 1997 Stage A
964.18	295.44	295.08	295.72
964.417	295.23	294.83	294.98
964.459	295.06	294.72	294.93
964.573	294.93	294.61	294.90
Swell head (ft)	0.51	0.47	0.82
X-Sec (RM)	Phase 1 - Condition 2		
964.18	320.81	320.91	321.54
964.417	320.43	320.01	320.64
964.459	319.75	319.67	319.25
964.573	319.75	319.47	319.40
Swell head (ft)	1.06	1.44	2.14

Table 4. Model Velocity Comparisons in feet per second for Phase 1.

	Phase 1 - Condition 1			
X-Sec (RM)	HEC-RAS	AdH 2012 Depth Avg	AdH 2012 Draft Depth	PM 1997 Stage A
964.18	4.05	3.64	3.98	5.31
964.417	4.96	5.28	5.77	7.90
964.459	5.76	5.56	6.08	7.90
964.573	5.42	5.23	5.72	7.34
X-Sec (RM)	Phase 1 - Condition 2			
964.18	6.33	6.84	7.66	6.42
964.417	7.55	9.68	10.84	9.26
964.459	9.68	10.14	11.35	12.73
964.573	8.41	9.58	10.73	10.47

Table 5. Water surface elevations (Ohio River Datum in feet) and swell head comparisons for Phase 2.

	Phase 2 - Condition 1		
X-Sec (RM)	HEC-RAS	AdH 2012	PM 1997 Stage B
964.18	295.79	295.39	295.82
964.417	295.50	295.11	295.35
964.459	294.74	294.55	294.92
964.573	294.93	294.47	294.95
Swell Head (ft)	0.86	0.92	0.87
X-Sec (RM)	Phase 2 - Condition 2		
964.18	321.15	321.87	320.81
964.417	320.73	321.02	320.43
964.459	319.24	319.96	319.52
964.573	319.75	319.23	319.83
Swell Head (ft)	1.40	2.64	0.98

Table 6. Model velocity comparisons for Phase 2 in feet per second.

	Phase 2 - Condition 1			
X-Sec	HEC-RAS	AdH 2012 Depth Avg	AdH 2012 Draft Depth	PM 1997 Stage B
964.18	4.59	3.82	4.18	4.21
964.417	5.57	5.39	5.89	6.09
964.459	8.53	8.11	8.86	7.71
964.573	5.95	5.38	5.89	6.58
X-Sec	Phase 2 - Condition 2			
964.18	6.63	5.58	6.26	5.76
964.417	7.83	8.55	9.60	7.03
964.459	12.04	12.04	13.52	10.00
964.573	8.60	9.87	11.06	7.65

Equally important for the velocity comparisons is the location of observation. All velocities were integrated over each cross section. The depth average velocities from AdH were compared to the HEC-RAS velocities. However, for the PM 1997 compared to AdH 2012, draft depth averaged velocities were computed and compared. The PM 1997 used weighted floats

drafted at 9.0 ft, thus the average draft depth velocities were used for proper comparison.

Since Phase 1 has a wider river pass width than Stage A, there are generally lower swell heads and lower velocities than those of HEC-RAS and PM 1997. This holds true for the WSEs, with the exception of the one upstream cross-section in the PM and the two downstream cross-sections in HEC-RAS for Condition 2 (see Table 7). Likewise, although not as consistent, the velocities are lower. Note that all AdH 2012 velocities are lower at the centerline cross-section, RM 964.459. Variations from the expected pattern for both velocities and WSEs at other cross-section locations are attributed to differences in models and bathymetry.

Table 7. Water surface elevation differences between models in feet.

	Phase 1 - Condition 1	
X-Sec (RM)	PM -AdH	HEC-RAS - AdH
964.18	0.64	0.36
964.417	0.15	0.40
964.459	0.21	0.34
964.573	0.29	0.32
	Phase 1 - Condition 2	
X-Sec (RM)	PM -AdH	HEC-RAS - AdH
964.18	0.63	-0.10
964.417	0.63	0.43
964.459	-0.42	0.08
964.573	-0.07	0.28
	Phase 2 - Condition 1	
X-Sec (RM)	PM -AdH	HEC-RAS - AdH
964.18	0.43	0.40
964.417	0.24	0.39
964.459	0.37	0.19
964.573	0.48	0.46
	Phase 2 - Condition 2	
X-Sec (RM)	PM -AdH	HEC-RAS - AdH
964.18	-1.06	-0.72
964.417	-0.59	-0.29
964.459	-0.44	-0.72
964.573	0.60	0.52

Phase 2 is slightly narrower than Stage B, thus the expectation is to produce a greater swell head and larger velocities through the pass. For Conditions 1 and 2, the swell head is greater with AdH; however, between adjacent cross sections, there is variability (see Table 7). The velocity through the cross-section at the centerline of the structure, RM 964.459, is greater than or equal to AdH and the other models with the exception of Condition 1. Again, variations from the expected pattern for both velocities and WSEs at other cross-section locations are attributed to differences in models and bathymetry.

4.4 Final dam configuration

The final dam configuration was simulated primarily for future work and validation purposes. If necessary, the final dam configuration could be used to evaluate sedimentation issues, mussel bed impacts, and navigation concerns. It also provides a comparison to the RMA-Z 2004 results and collected field data along with the PM 1997 results. The RMA-Z 2004 model simulated the finished dam in an open river condition.

The USGS report also provided field data that had been collected. Fifteen ADCP cross-sections were measured for velocities. The cross sections are in ascending order from upstream (see Figure 22). The flow during the field collection effort was 770,000 cfs at a tailwater of 322.4 ft, (Ohio River Datum). From the field data and models, a cross-section averaged velocity was calculated (see Figure 23). Close agreement is shown between AdH 2012 and the field data. The data from AdH 2012 followed the same pattern as the field data with an average error of 4.0 percent and a maximum and minimum error of 9.0 percent and 0.8 percent, respectively. This provided a reasonable level of assurance to the validity of the AdH 2012 results. A 72,000 cfs event was also collected by the USGS; however, this flow was significantly lower than Condition 1 (350,000 cfs) for this modeling effort, therefore, a comparison was not considered valid.

The PM 1997 data were also used for comparison. In the PM 1997, a 270,000 cfs flow was run at a tailwater elevation of 293.7 ft for the final dam configuration. The PM 1997 results were overlaid with the AdH 2012 results in Figure 24. The black vectors with the scalar quantities represent the PM 1997 while the transparent color-filled contours and purple vectors represent the AdH 2012 results. Both models agree in magnitude and direction for the velocity field. The only variation is the return flow from an eddy downstream of the tainter gates. This eddy was not replicated in

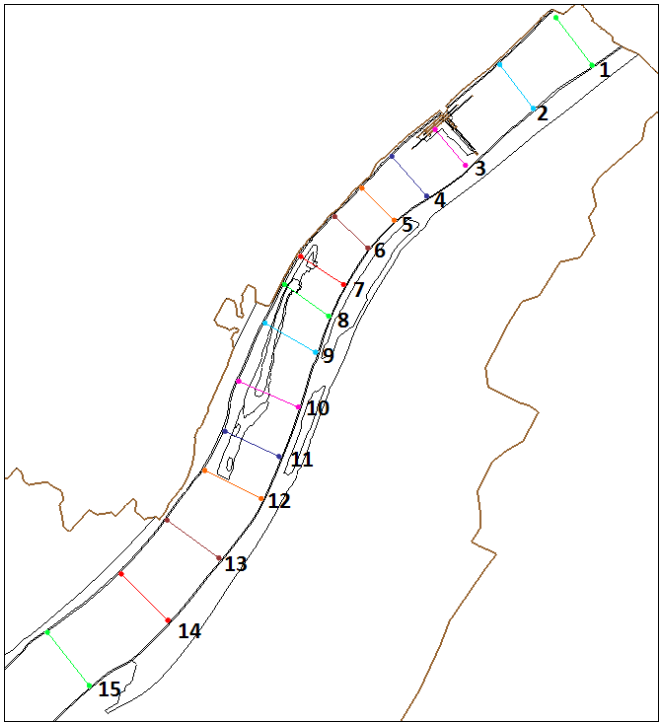

Figure 22. US Geological Survey field survey and model cross-section locations.

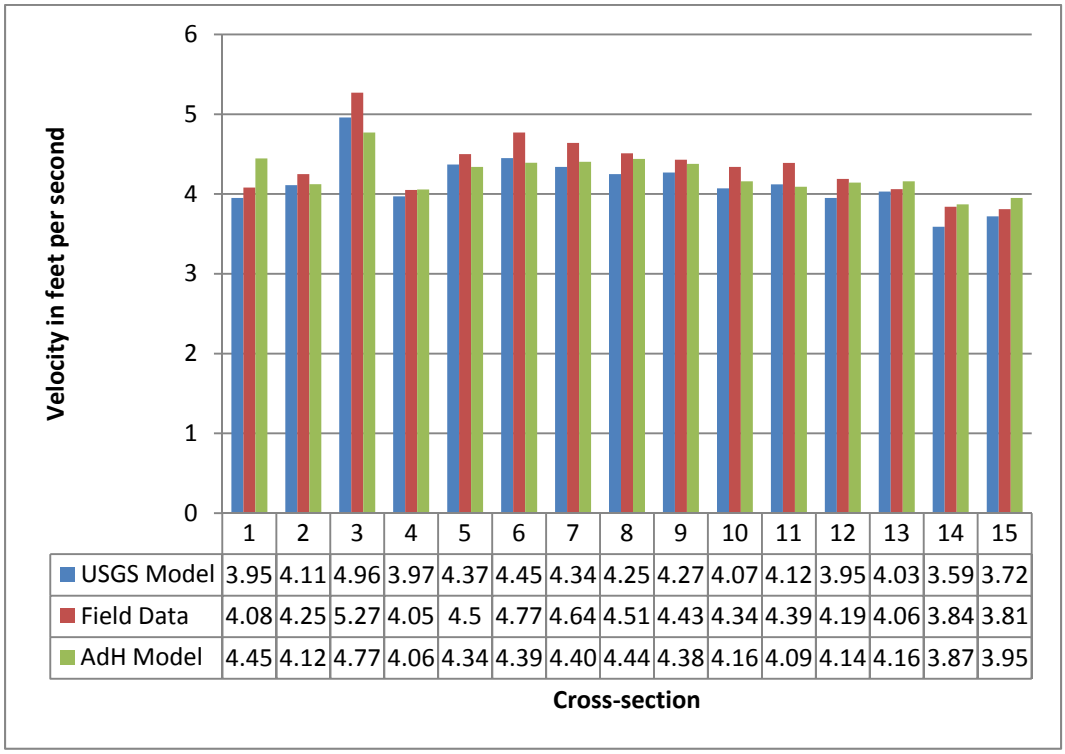

	1	2	3	4	5	6	7	8	9	10	11	12	13	14	15
USGS Model	3.95	4.11	4.96	3.97	4.37	4.45	4.34	4.25	4.27	4.07	4.12	3.95	4.03	3.59	3.72
Field Data	4.08	4.25	5.27	4.05	4.5	4.77	4.64	4.51	4.43	4.34	4.39	4.19	4.06	3.84	3.81
AdH Model	4.45	4.12	4.77	4.06	4.34	4.39	4.40	4.44	4.38	4.16	4.09	4.14	4.16	3.87	3.95

Figure 23. Average velocity comparison for USGS TABS, AdH 2012, and field data.

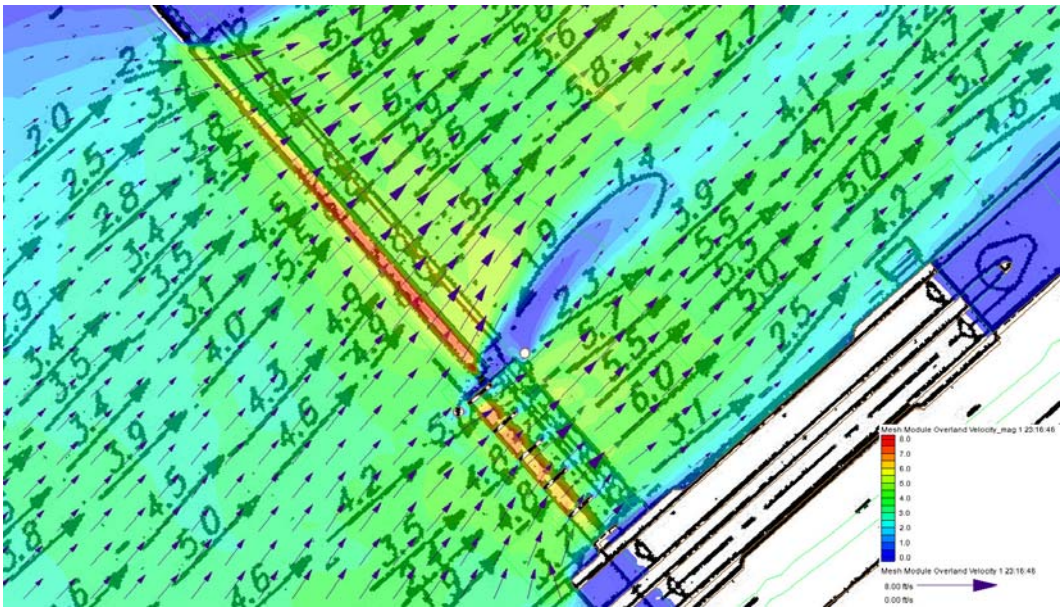

Figure 24. PM 1997 and AdH 2012 comparison.

AdH; however, the shadow from the blockage is replicated and aligns with the return eddy of the PM 1997. The following factors might be the reason for the absence of the eddy in AdH 2012:

- Three-dimensional effects are captured in the physical model.
- Different bathymetries were used for both models.
- Upstream dikes were in place for the PM 1997.
- AdH 2012 has a cell upstream and downstream of the last tainter gate pier and the PM 1997 does not.
- Scaling effects in the result for the PM 1997.

By capturing the shadow of the blockage in AdH, it is believed that the appropriate flow distribution is captured in the model. The agreement between the two models provides additional confidence in the AdH 2012 results.

5 Results

The aforementioned boundary conditions (Chapter 3) were run for Phase 1, Phase 2, and the final dam configuration. With every test case, WSE, depth, velocity, bed shear, and WSE cross-section were plotted (Figures 25-50). Each plan view figure (WSE, depth, velocity, and bed shear) was generated in SMS and only includes the local area around the Olmsted structures. The WSE cross-sections that correspond to HEC-RAS cross-sections through the navigation pass are plotted to show the 2D aspects of flow around the structure.

The velocity magnitude figures are the depth averaged value, but are not the velocities used in the STS. The velocities for the STS were calculated using the Law of the Wall Theory derived by Millikan (1938) and Isakson (1937) and the depth-averaged velocity from AdH 2012. The log velocity profile was simply integrated over the draft depth of the design vessel (9.0-ft) to produce a representative impacting velocity on the vessel for use in the STS.

$$\frac{U}{u_*} = \frac{1}{k} ln \frac{z}{K} + A \tag{3}$$

where

U = The velocity at depth z,
u_* = The square-root of bed shear divided by density,
k = The von Karman constant,
K = The bed roughness height, and
A = A constant.

This is referred to as the draft depth averaged velocity.

The bed shear stress values were post processed using the depth and depth averaged velocity calculated by AdH 2012. Using the shear stress and Manning's equations:

$$\tau = \rho g h S \tag{4}$$

$$V = \frac{1.486}{n} h^{2/3} S^{1/2} \tag{5}$$

The following equation was derived for bed shear:

$$\tau = C\frac{V^2}{h^{1/3}} \quad (6)$$

where

V = The depth averaged velocity,
h = The flow depth,
C = A constant (when n is 0.02 or 0.03 C is 0.0113 or 0.0254 respectively),
τ_o = Bed shear,
τ = Shear stress,
n = Manning's number,
S = The energy slope,
g = Gravity, and
ρ = Fluid density.

5.1 Phase 1

Both flow conditions for the Phase 1 cofferdam were as expected. Water surface elevations showed a swell head as flow passed the structure, and the appropriate behavior of the floating guard-walls drafting at 11-ft (see Figures 25 and 26). Depth-averaged and draft depth velocities bed shear stresses peaked through the navigation pass and directly above the rock dike (see Figure 27 - 29). Figures 30 and 31 show the location and super elevation of the WSE through the navigation pass illustrating the two-dimensional nature of the flow field. Figures 32 through 37 show the same output for Condition 2. (Note: scales change with different figures).

5.2 Phase 2

Phase 2 evaluations were the same as those for Phase 1 (see Figures 38 through 50). Water surface elevations showed a swellhead as flow passed the structure, and the appropriate behavior due to the floating guard-walls drafting at 11-ft. Depth-averaged velocities peaked through the navigation pass above the wicket gates. However, Phase 2 cofferdam conditions produced vortex shedding on the downstream side of the cofferdam as discussed previously.

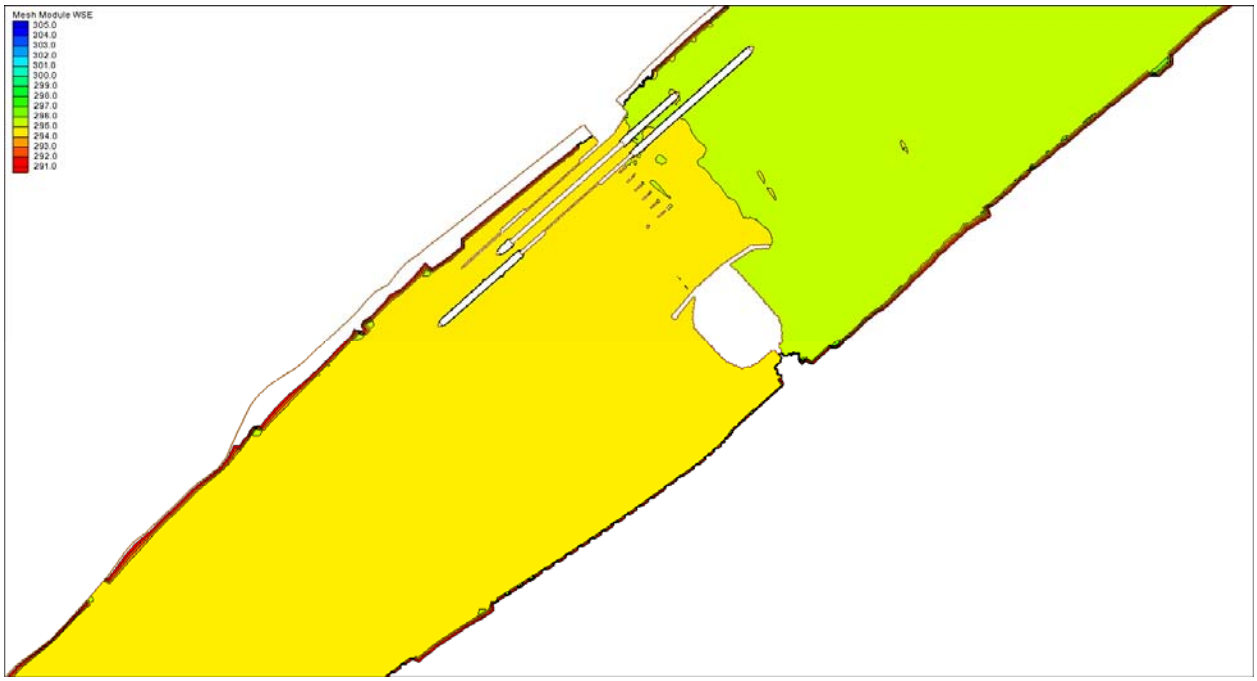

Figure 25. Water surface elevation in feet above the Ohio River Datum for Condition 1.

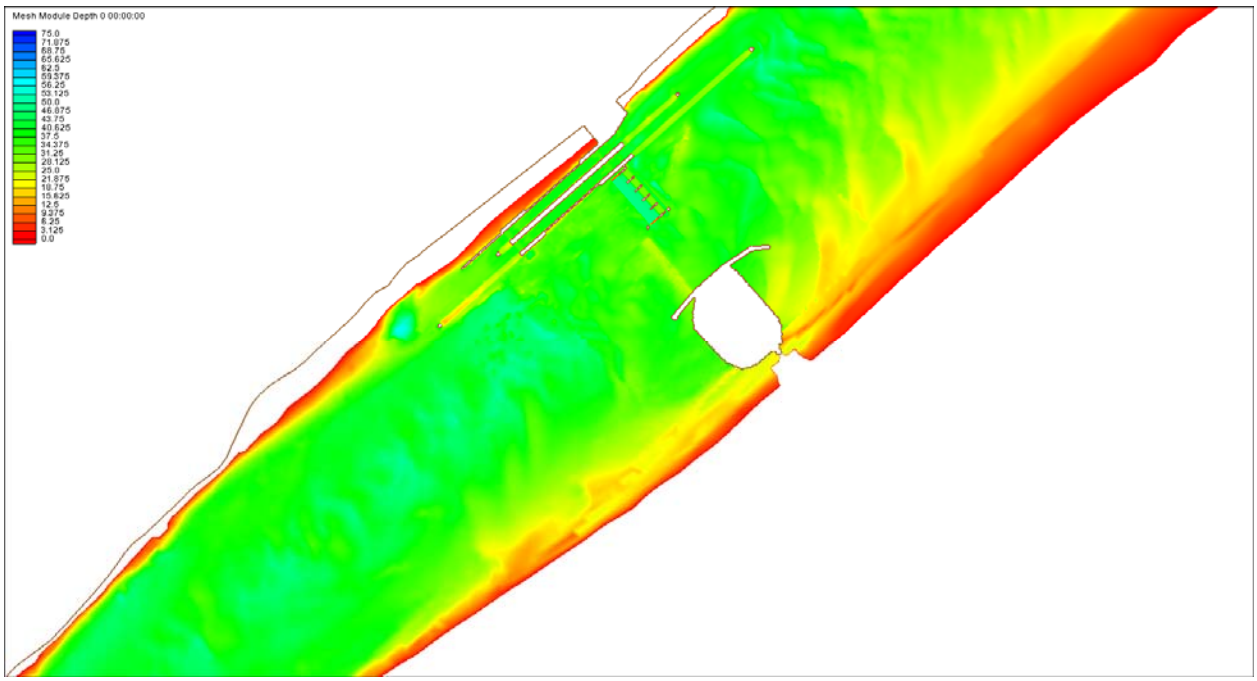

Figure 26. Depth in feet for Condition 1.

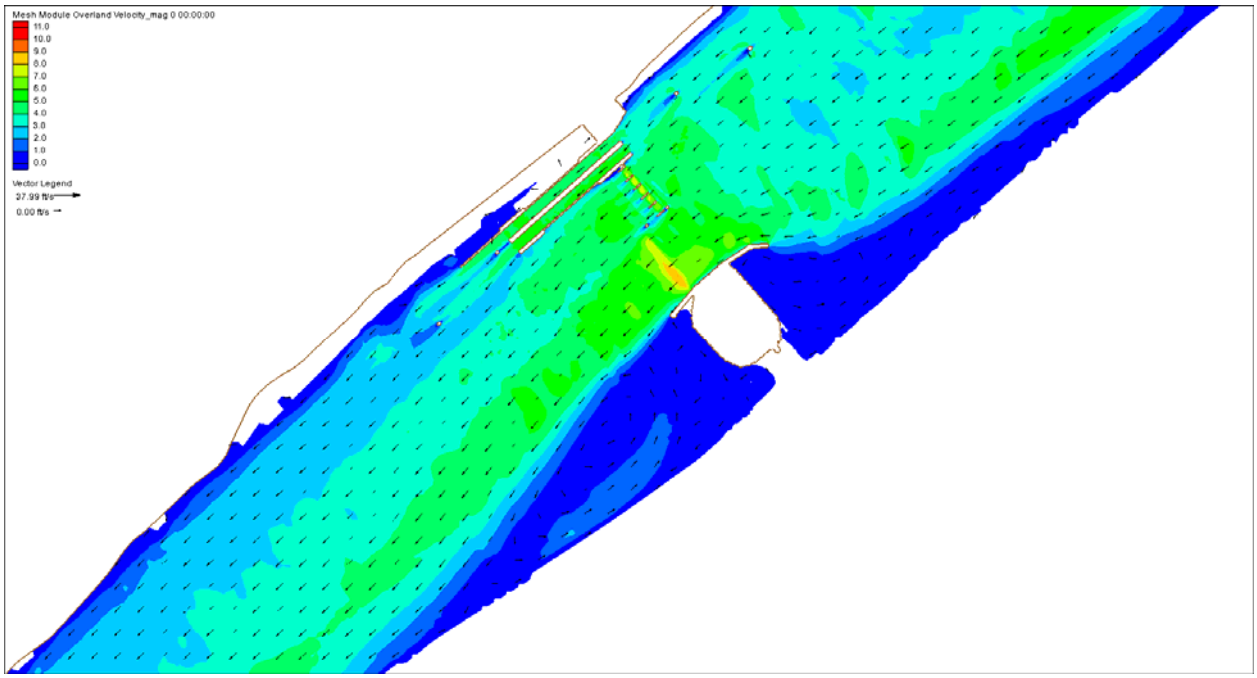

Figure 27. Depth-averaged velocity magnitude in feet per second for Condition 1.

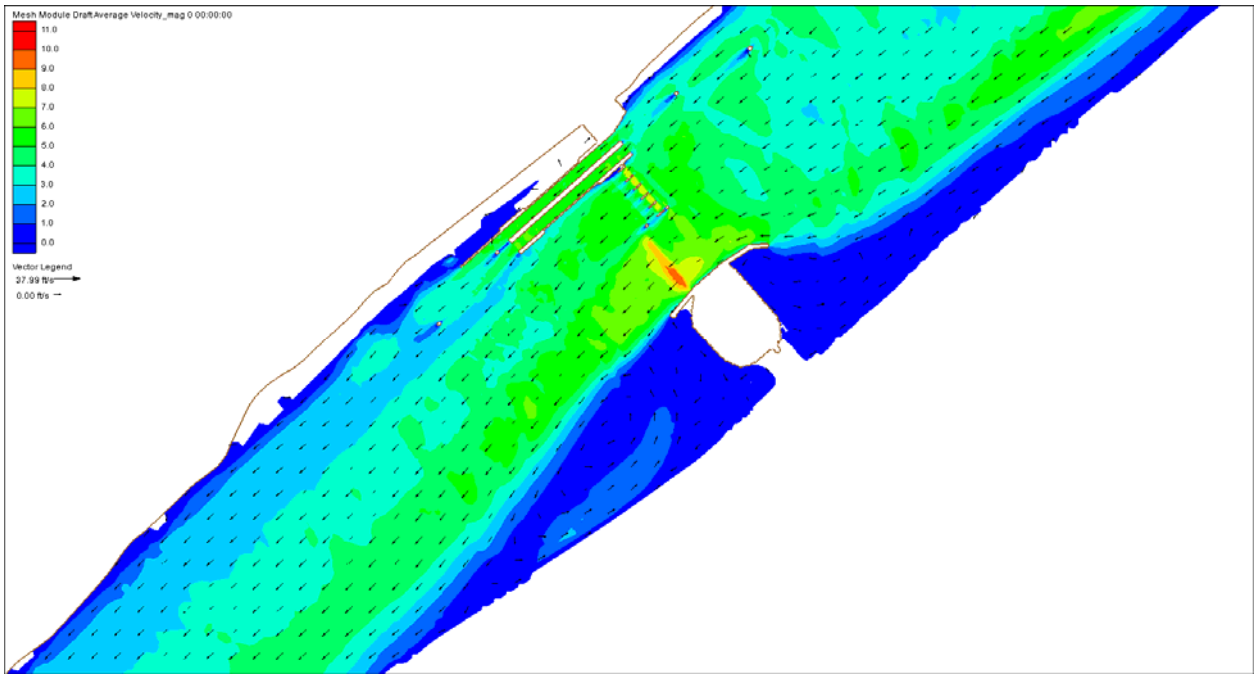

Figure 28. Draft depth-averaged velocity magnitude in feet per second for Condition 1.

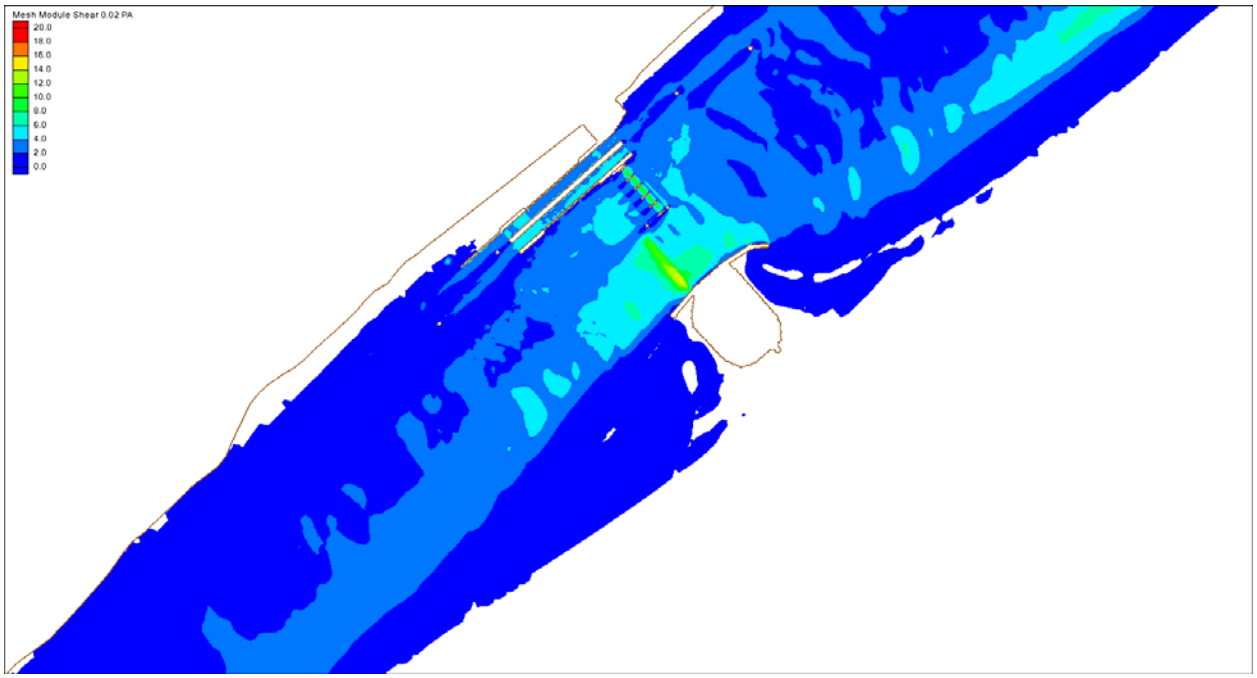

Figure 29. Bed shear stress in Pascals for Condition 1.

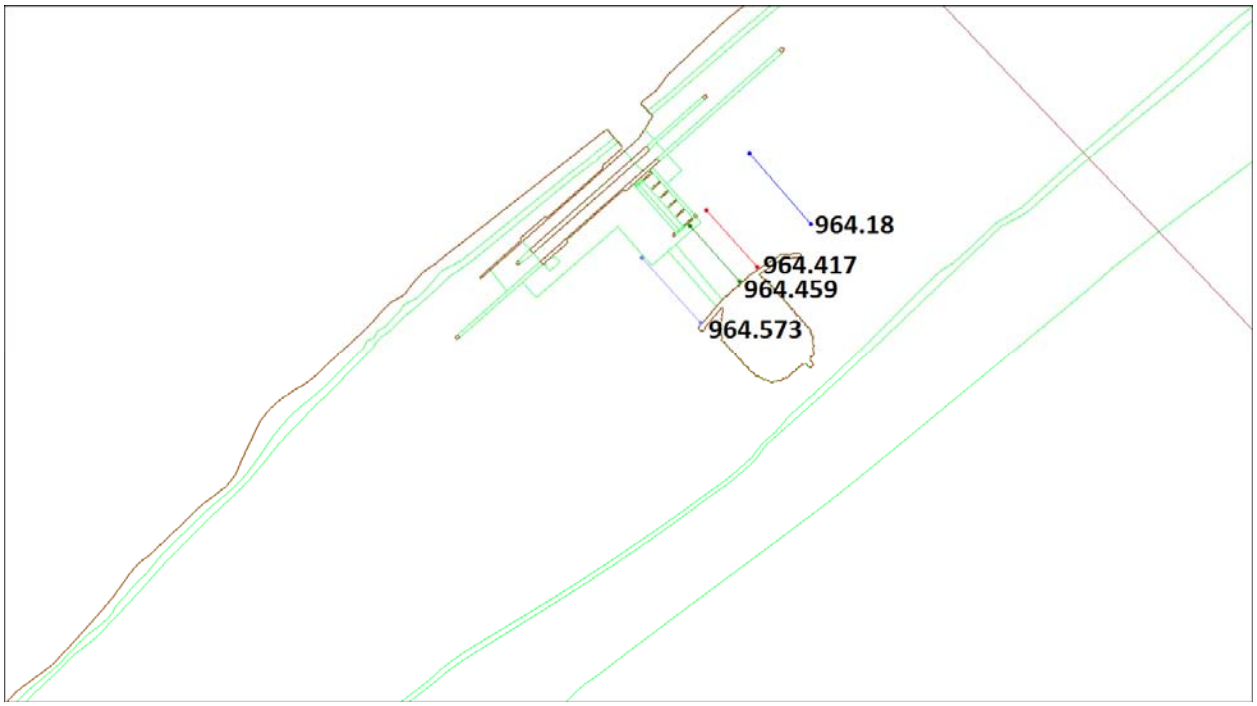

Figure 30. HEC-RAS cross-section locations in the AdH 2012.

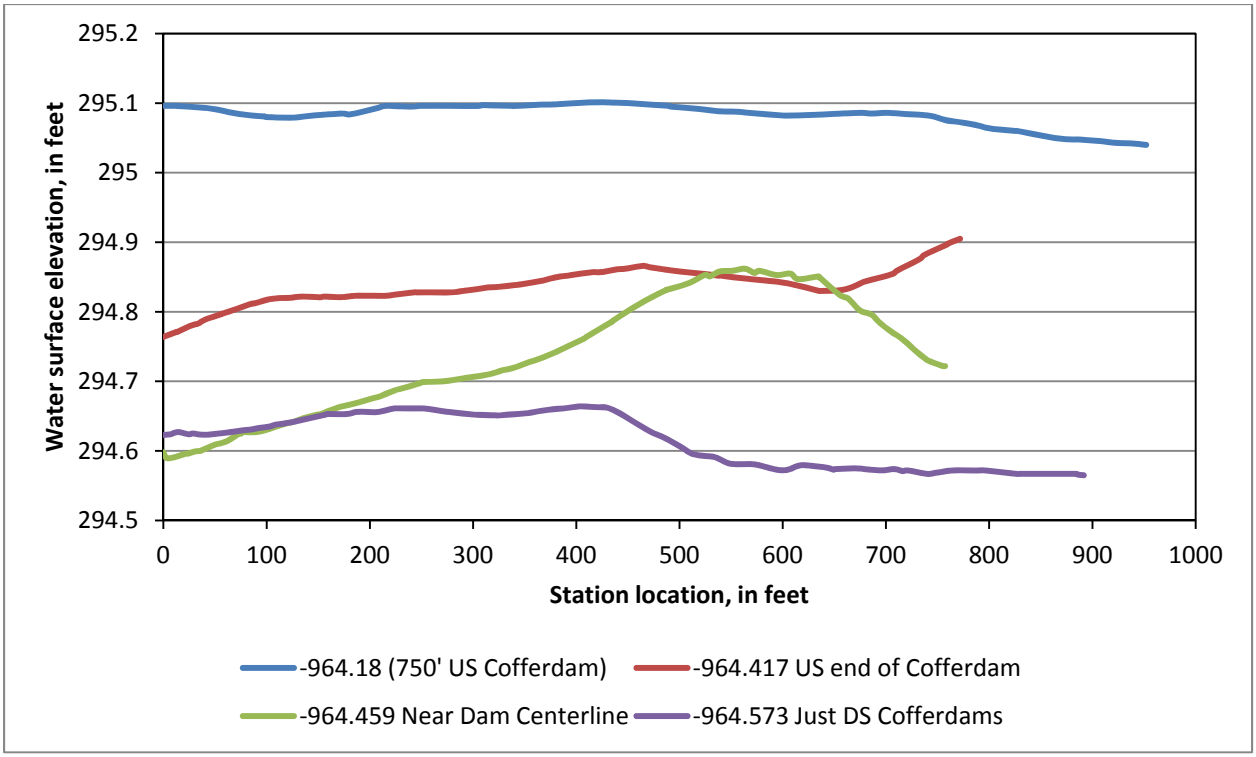

Figure 31. Water surface elevation cross sections through the navigation pass (Condition 1).

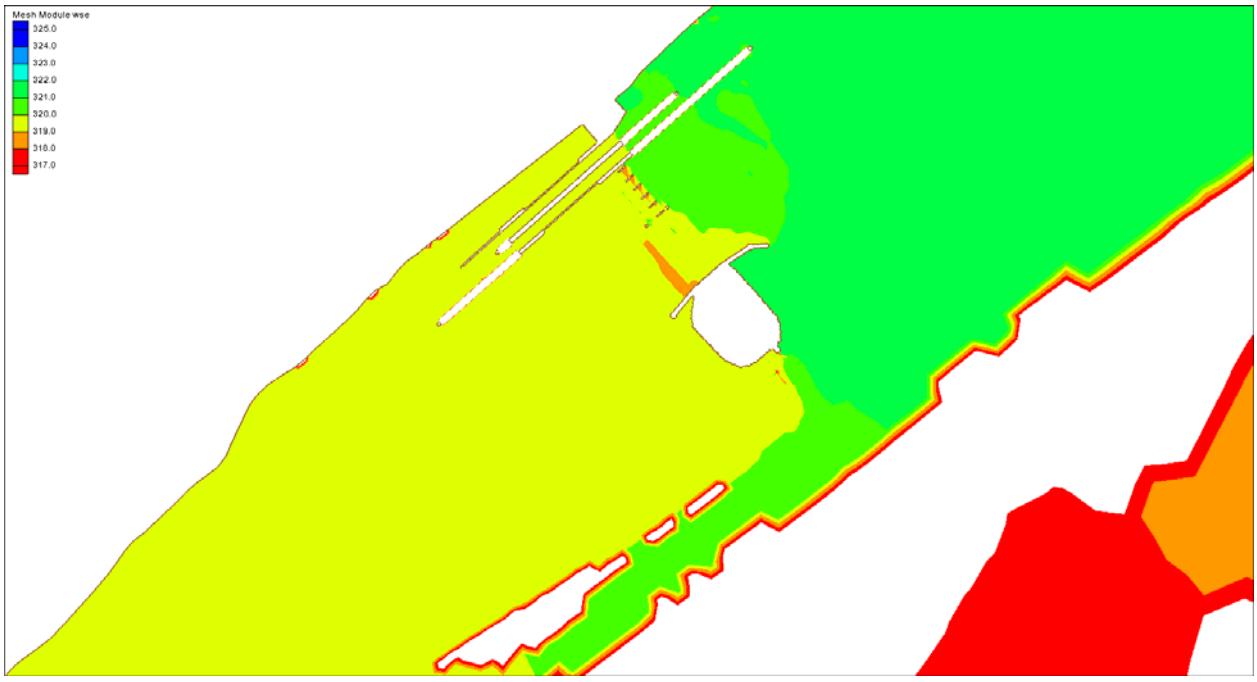

Figure 32. Water surface elevation in feet above the Ohio River Datum for Condition 2.

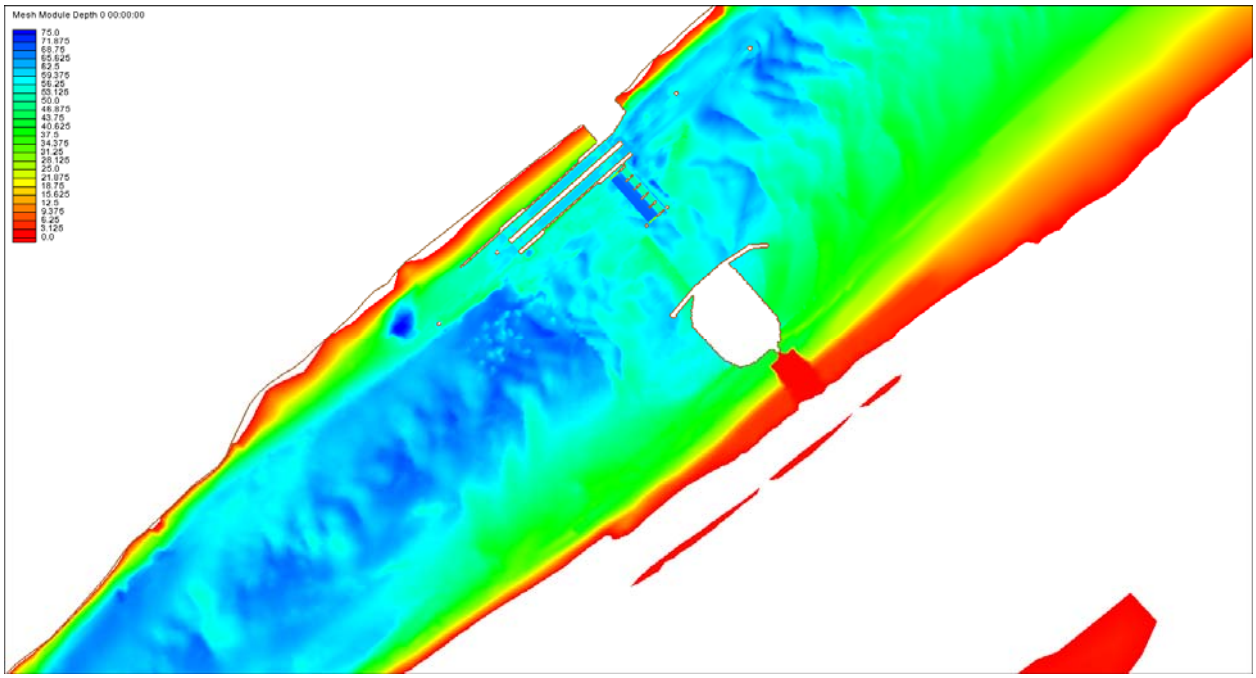

Figure 33. Depth in feet for Condition 2.

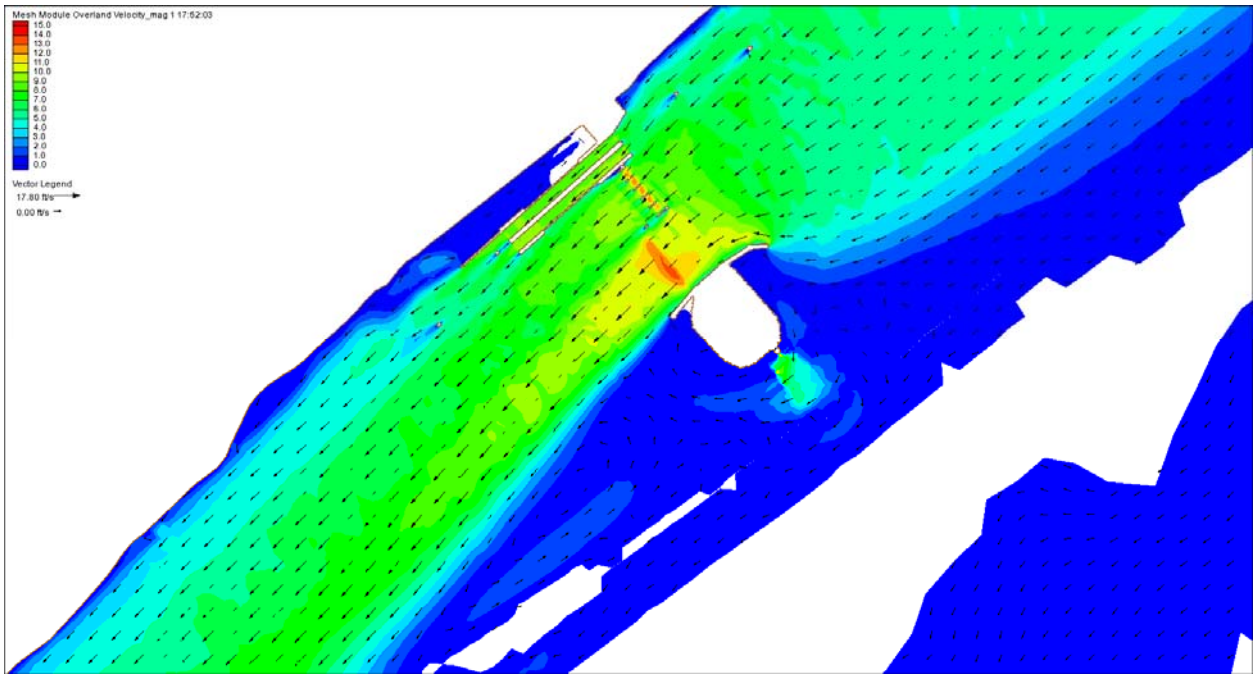

Figure 34. Depth-averaged velocity magnitude in feet per second for Condition 2.

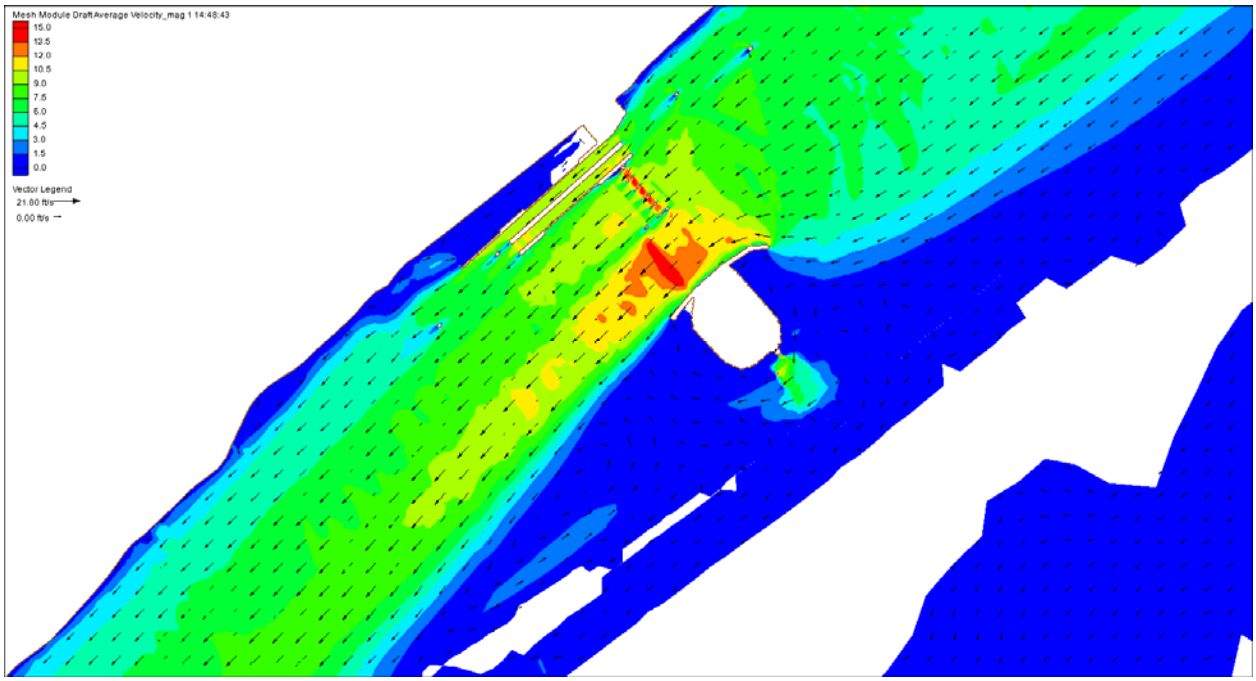

Figure 35. Draft depth-averaged velocity magnitude in feet per second for Condition 2.

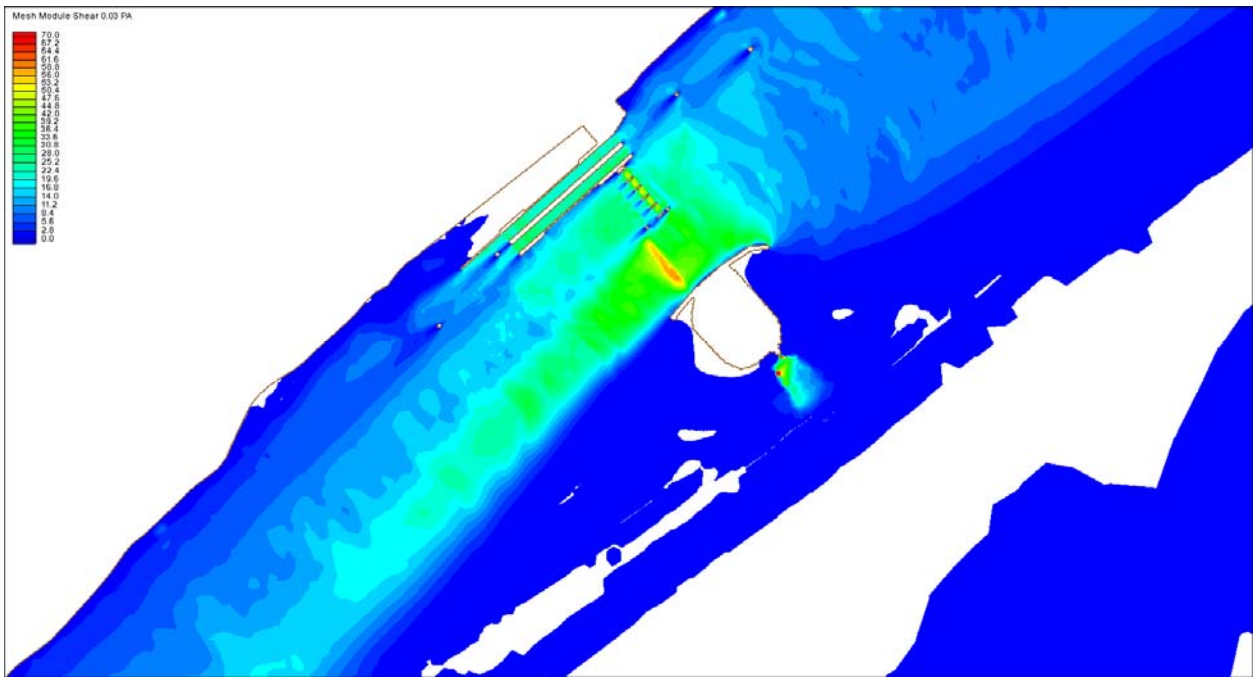

Figure 36. Bed shear in Pascals for Condition 2.

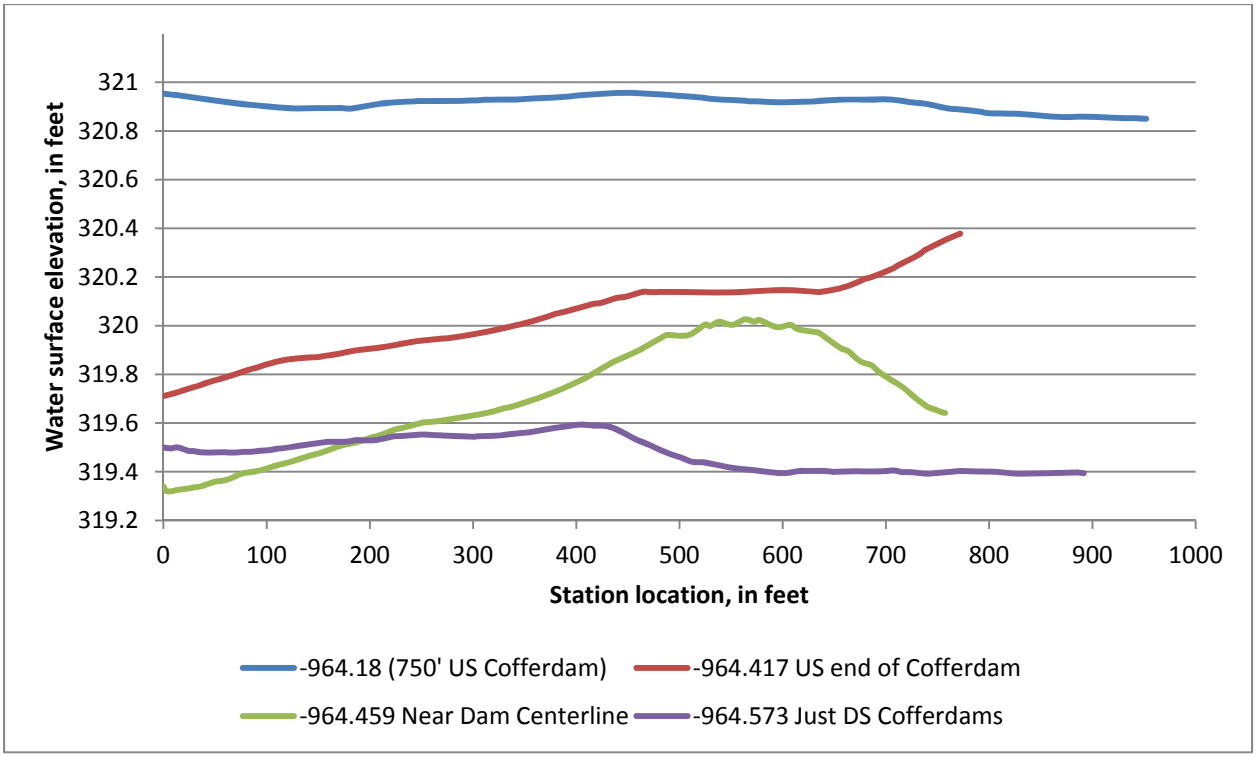

Figure 37. Water surface elevation cross sections through the navigation pass (Condition 2).

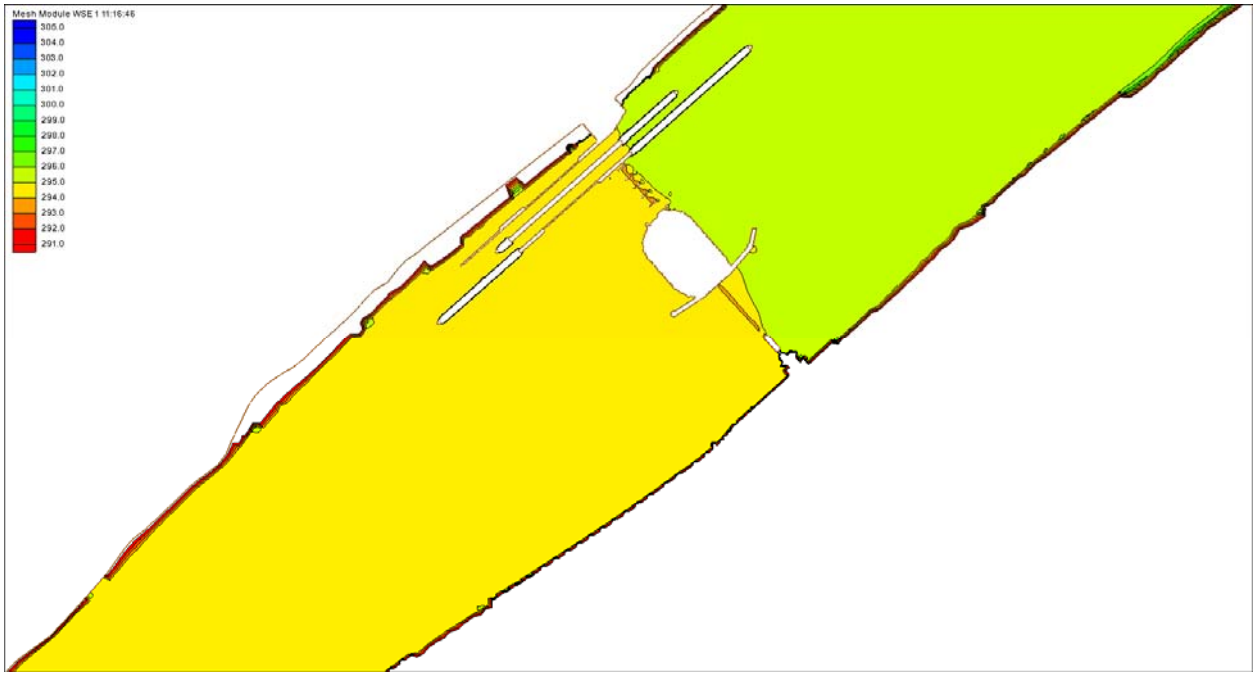

Figure 38. Water surface elevation in feet above the Ohio River Datum for Condition 1.

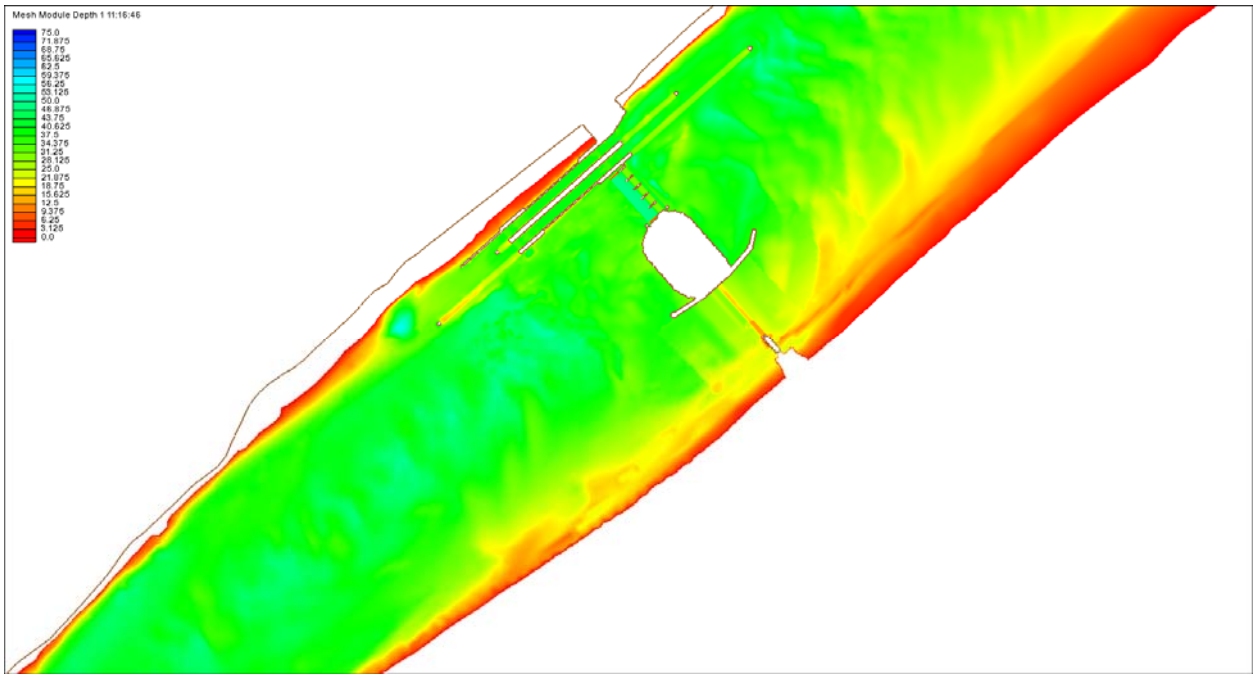

Figure 39. Depth in feet for Condition 1.

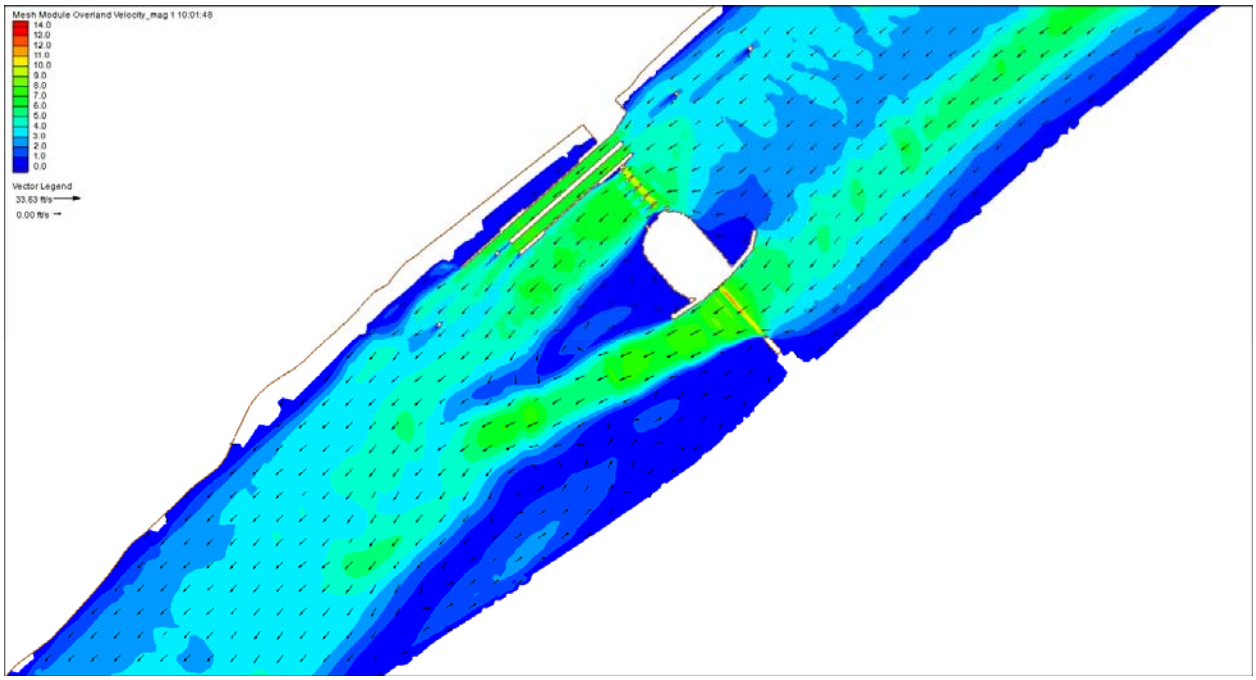

Figure 40. Depth-averaged velocity magnitude in feet per second for Condition 1 (typical).

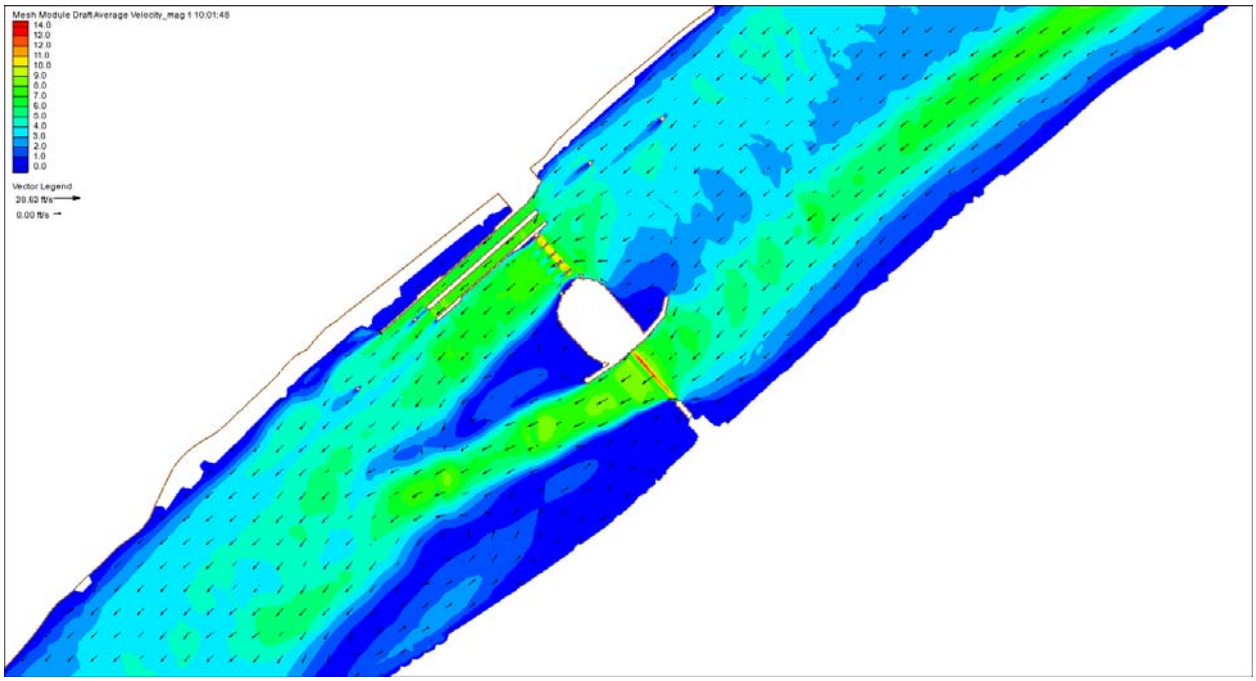

Figure 41. Draft depth velocity magnitude in feet per second for Condition 1 (typical).

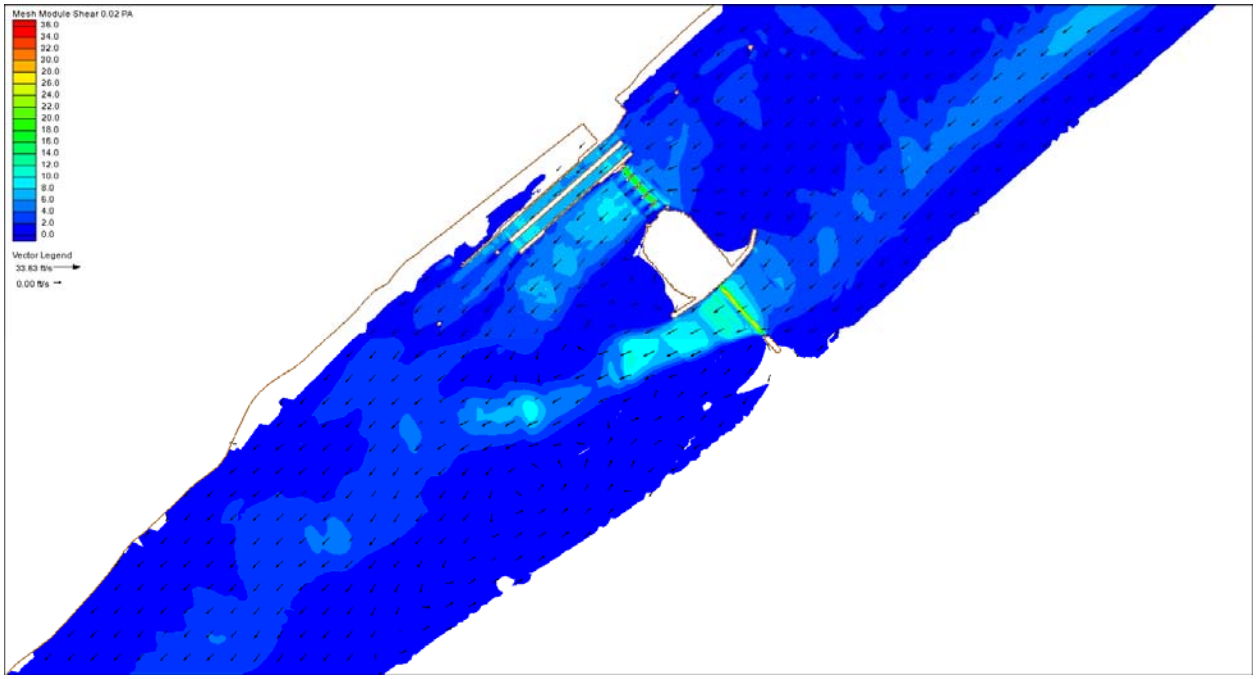

Figure 42. Bed shear stress in Pascals for Condition 1 (typical).

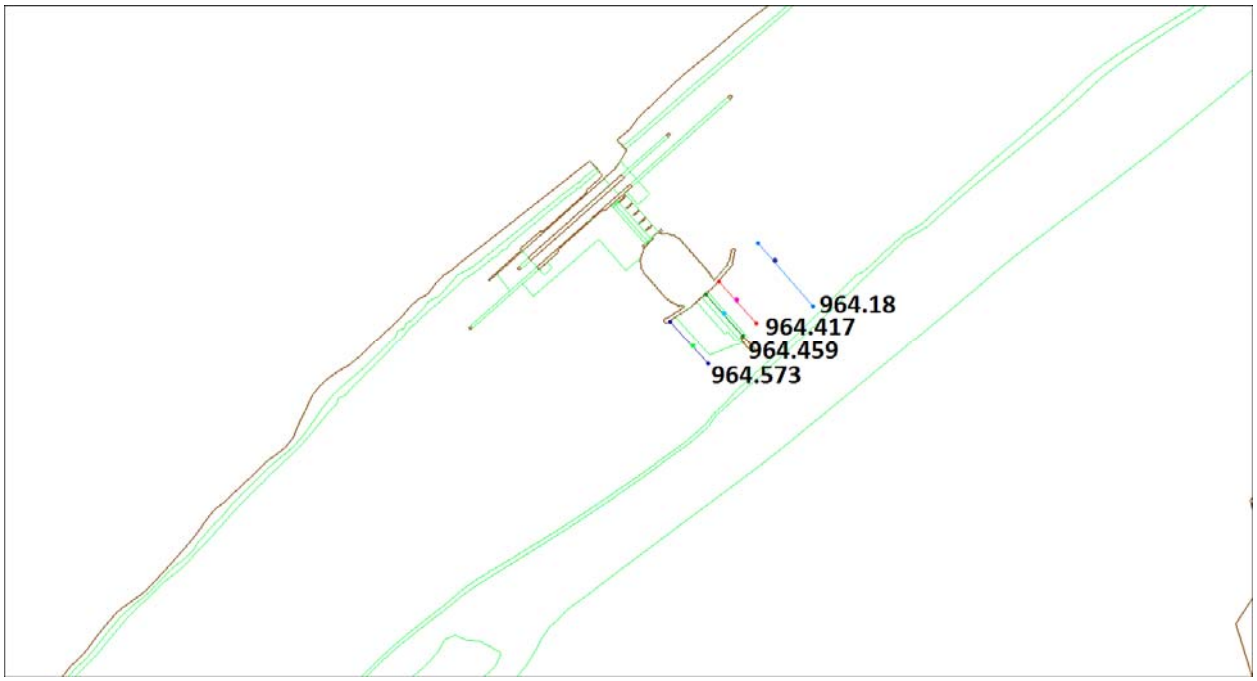

Figure 43. HEC-RAS cross-section locations in the AdH 2012.

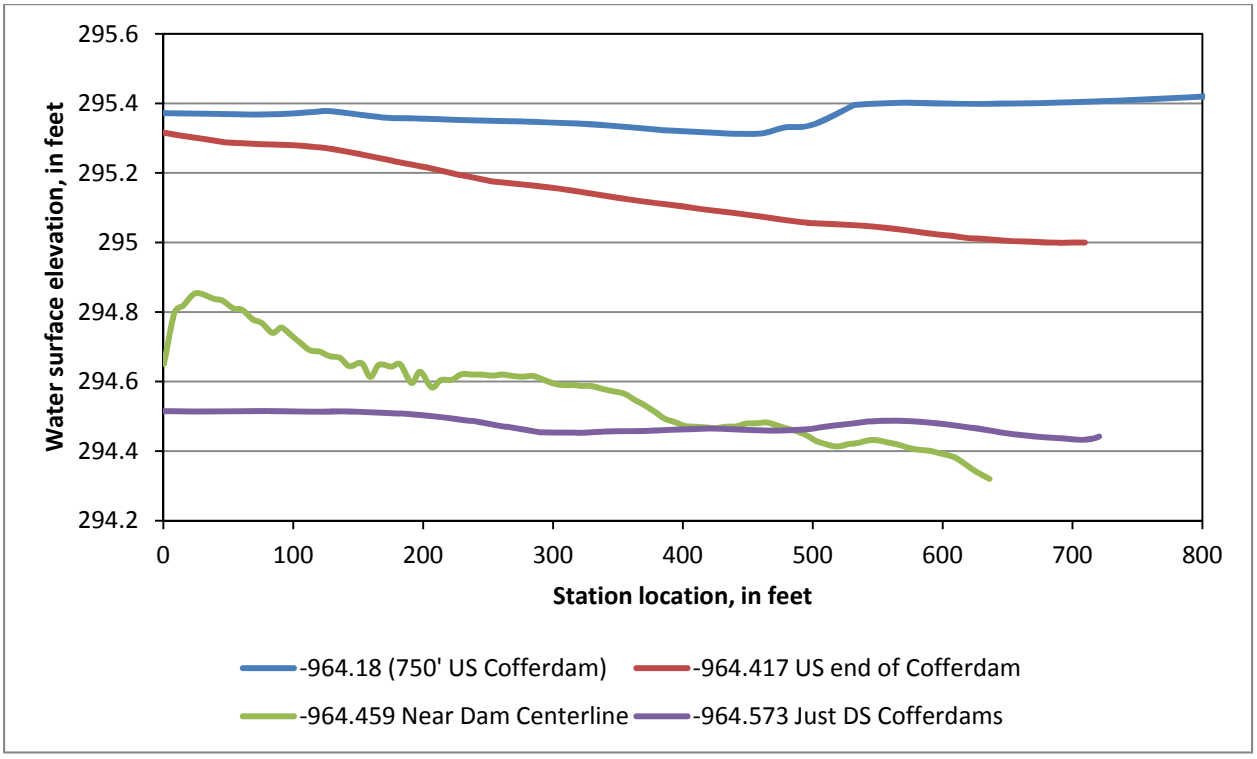

Figure 44. Water surface elevation cross sections through the navigation pass (Condition 1).

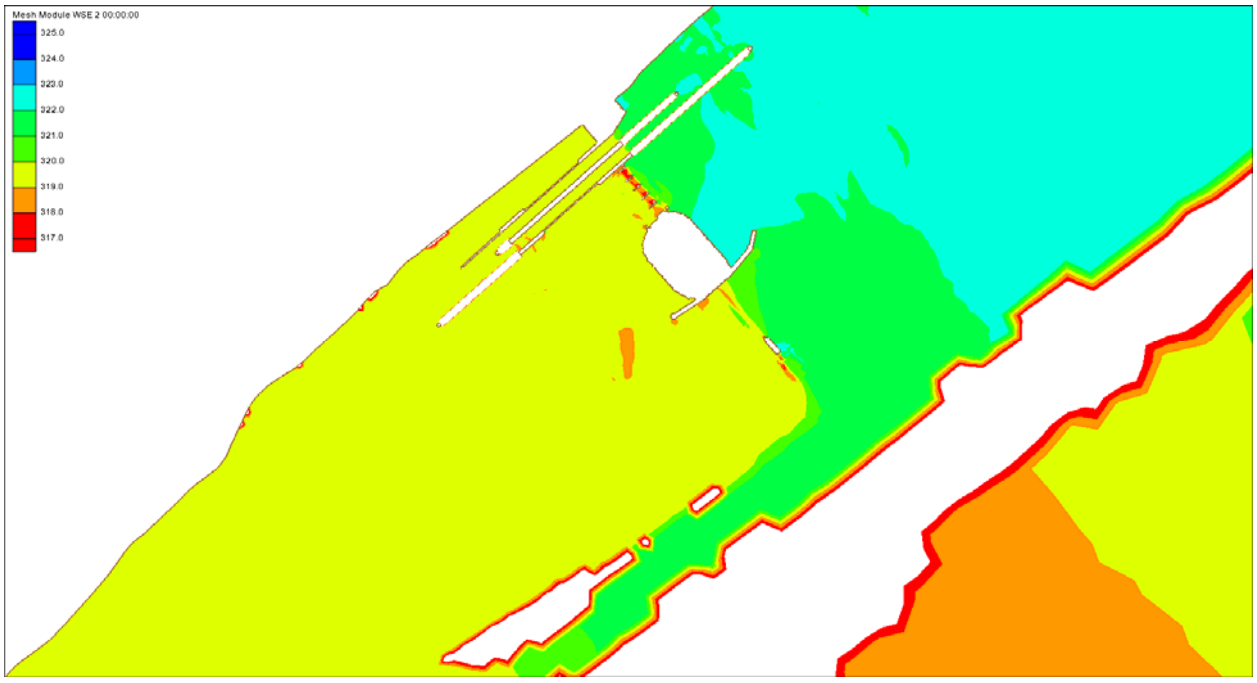

Figure 45. Water surface elevation in feet above the Ohio River Datum for Condition 2.

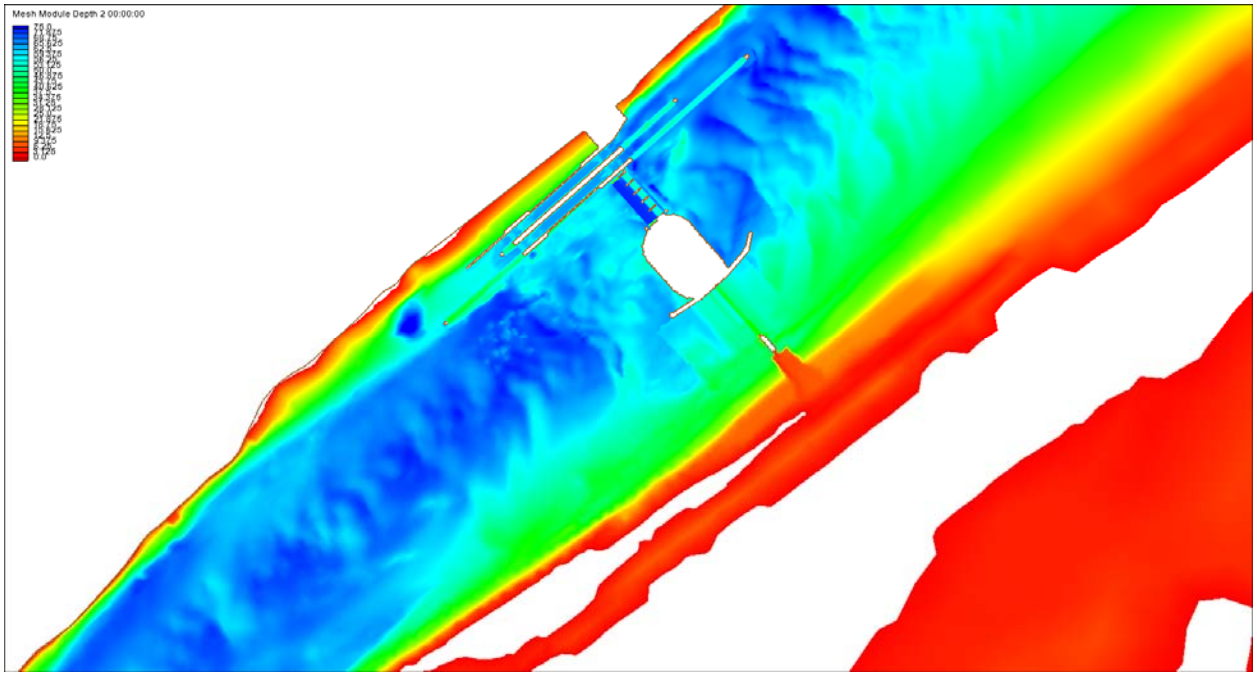

Figure 46. Depth in feet for Condition 2.

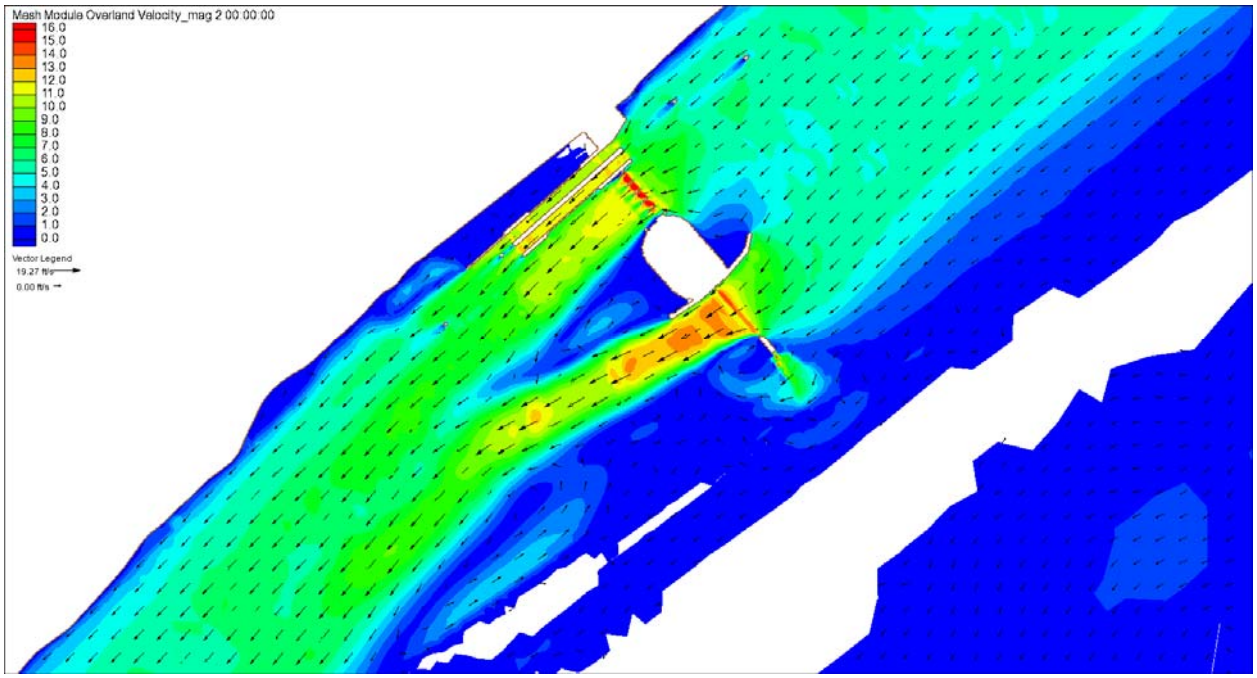

Figure 47. Depth-averaged velocity magnitude in feet per second for Condition 2 (typical).

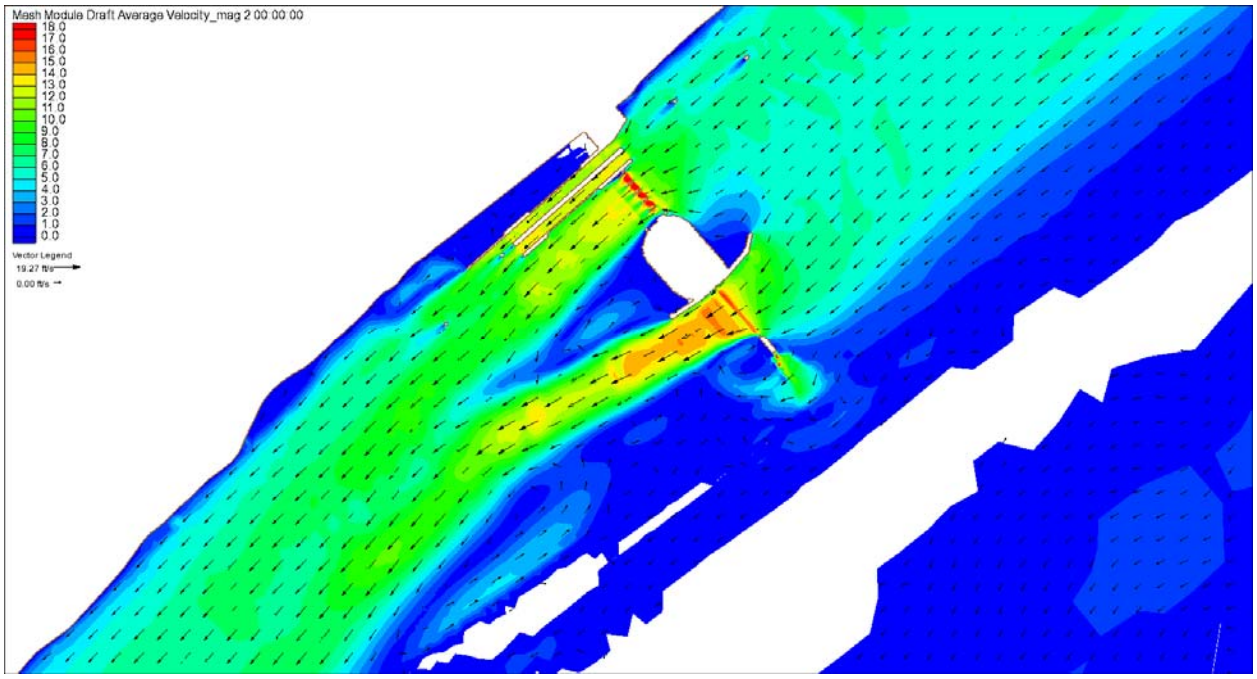

Figure 48. Draft depth velocity magnitude in feet per second for Condition 2 (typical).

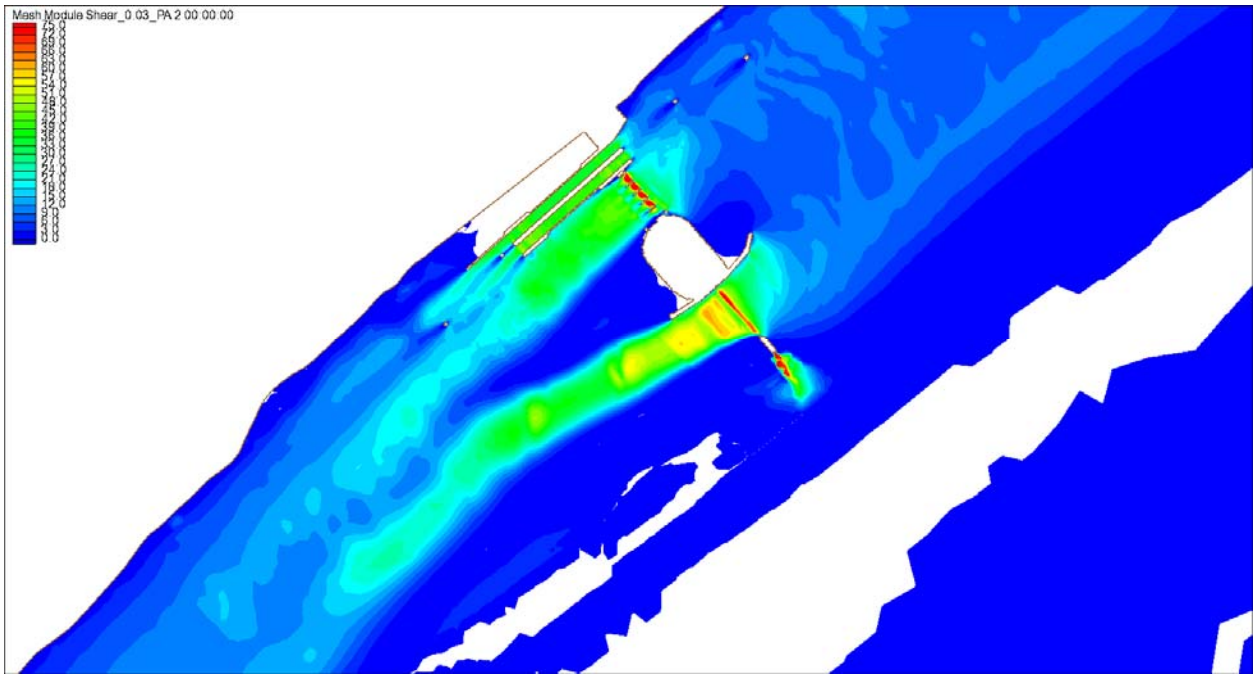

Figure 49. Bed shear stress in Pascals for Condition 2 (typical).

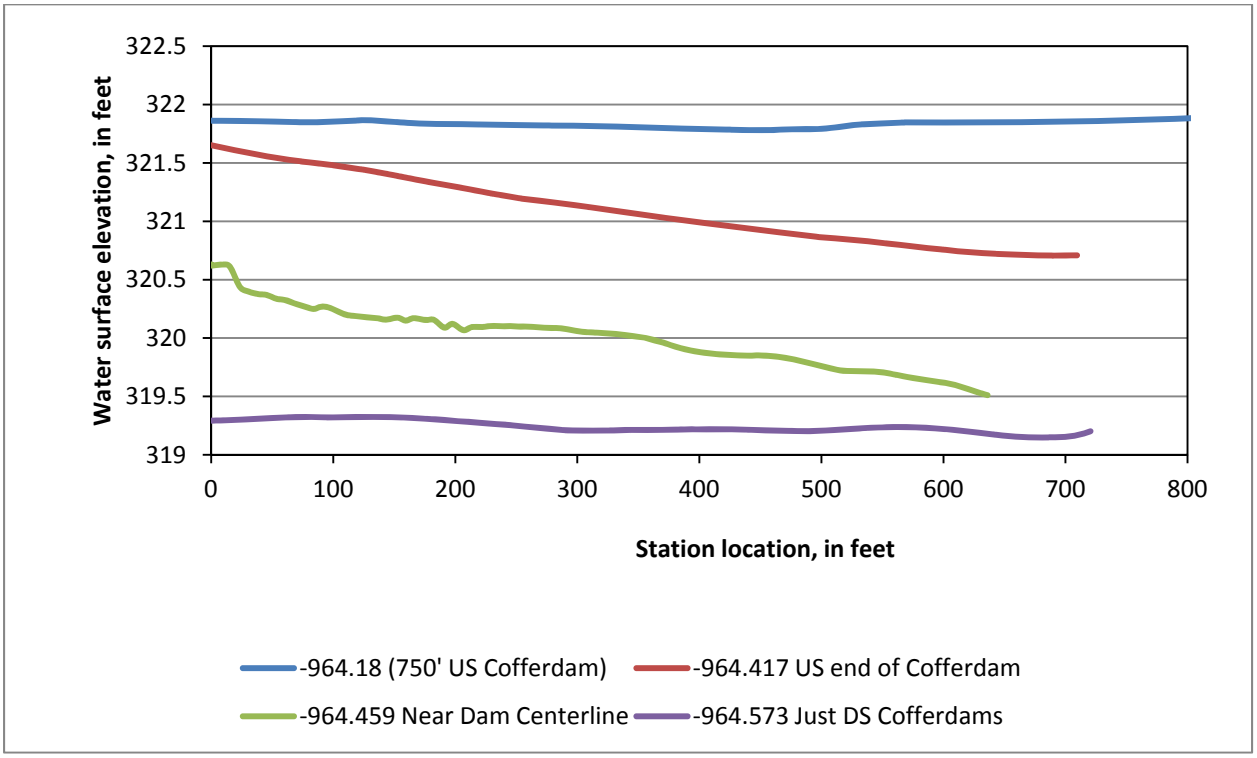

Figure 50. Water surface elevation cross sections through the navigation pass (Condition 2).

5.3 Pressure field simulations

At each of the twelve intersecting points of the boat paths and cross sections previously discussed, for both cofferdam phases, the peak velocity was recorded. The peak velocity typically occurred as the vessel's bow crossed the cross-section line. A difference between the velocity profile before the bow of the vessel crossed the cross-section and as the bow crossed the cross-section was recorded. An example of this is shown in Figure 51. From these peaks a spatially interpolated difference map was generated using a distance weighted average scheme (see Figures 52 – 55). The differences were then added to the existing velocities (no boat pressure field simulations) increasing all the velocities through the navigation passes. This was done to ensure that the result in the ship simulator included the impact of the vessel on the currents irrespective of the boat's location in the structure.

5.4 Final dam configuration

Conditions 1 and 2 were run with the final dam configuration. Figures 56 and 57 show the depth averaged velocities.

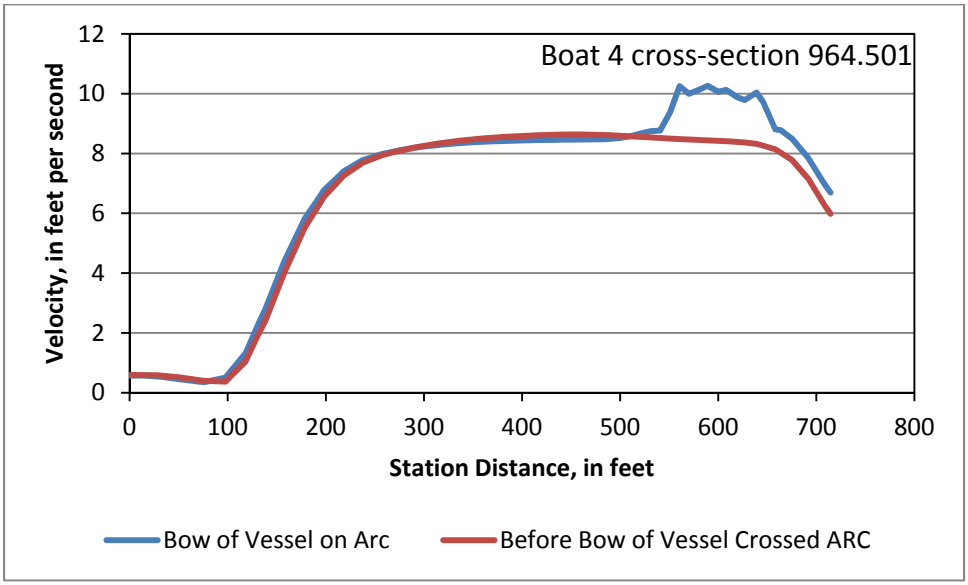

Figure 51. Cross section as the pressure field passes over.

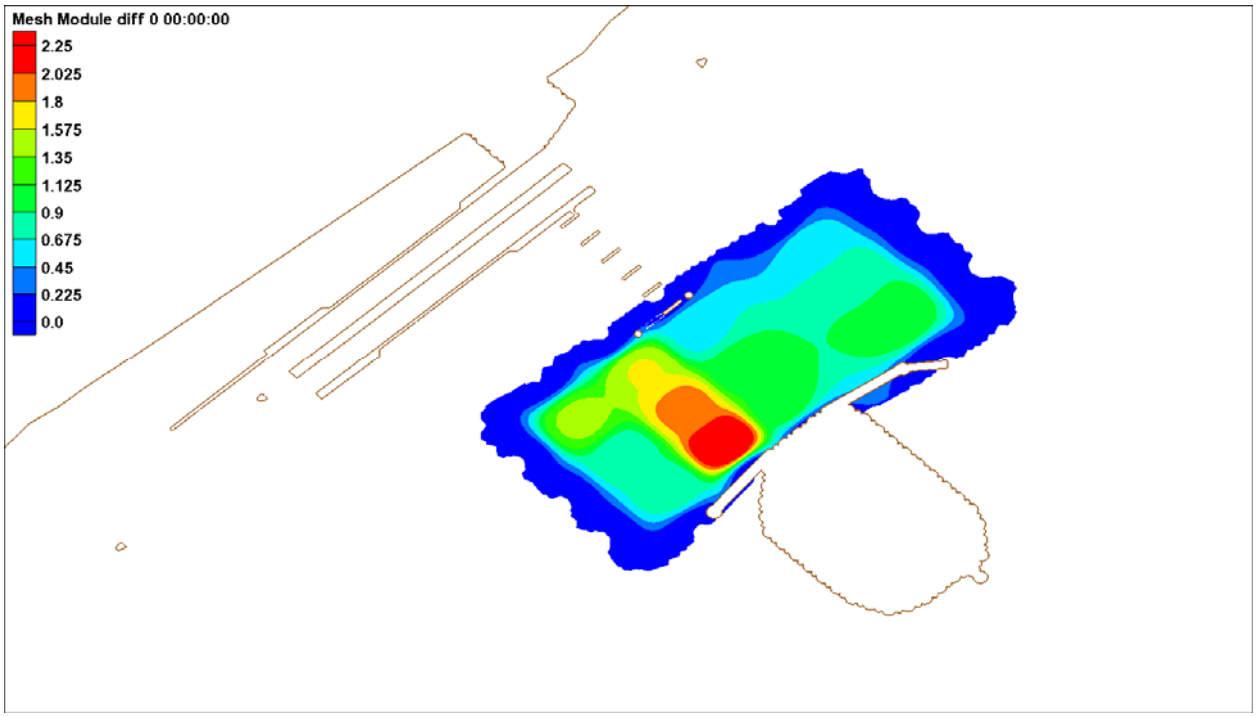

Figure 52. Phase 1-Condition 1 velocity magnitude difference.

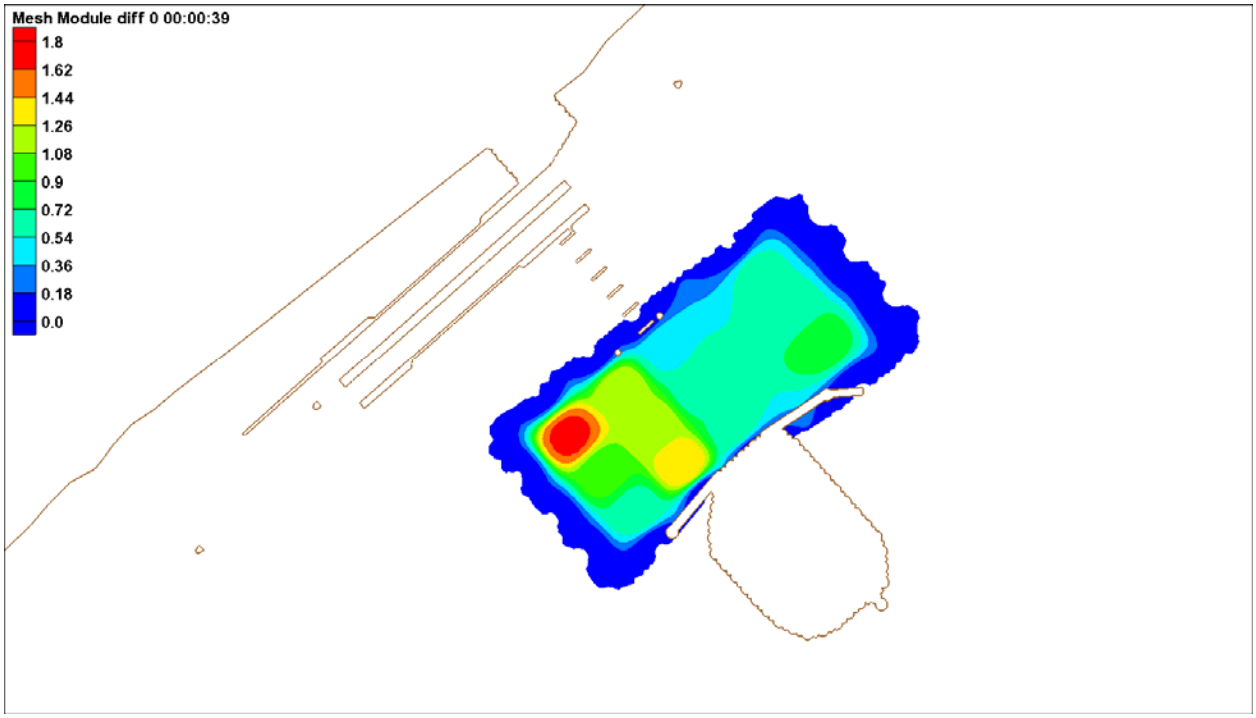

Figure 53. Phase 1-Condition 2 velocity magnitude difference.

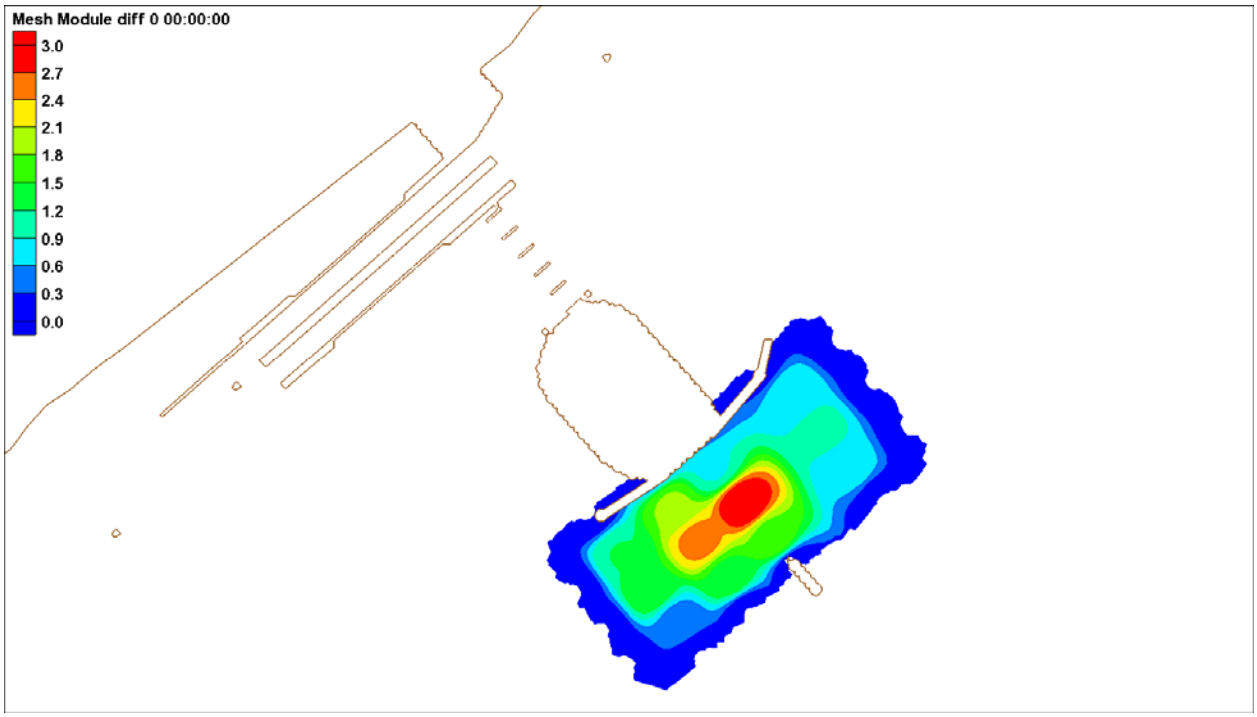

Figure 54. Phase 2-Condition 1 velocity magnitude difference.

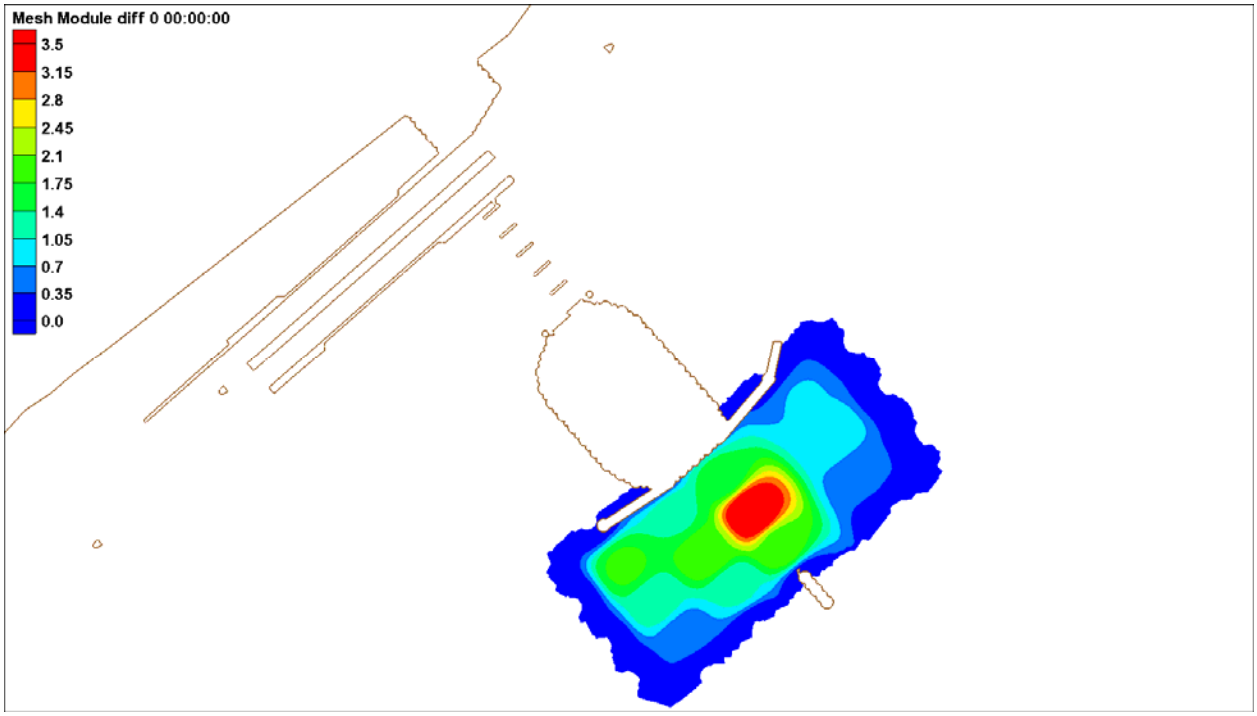

Figure 55. Phase 2-Condition 2 velocity magnitude difference.

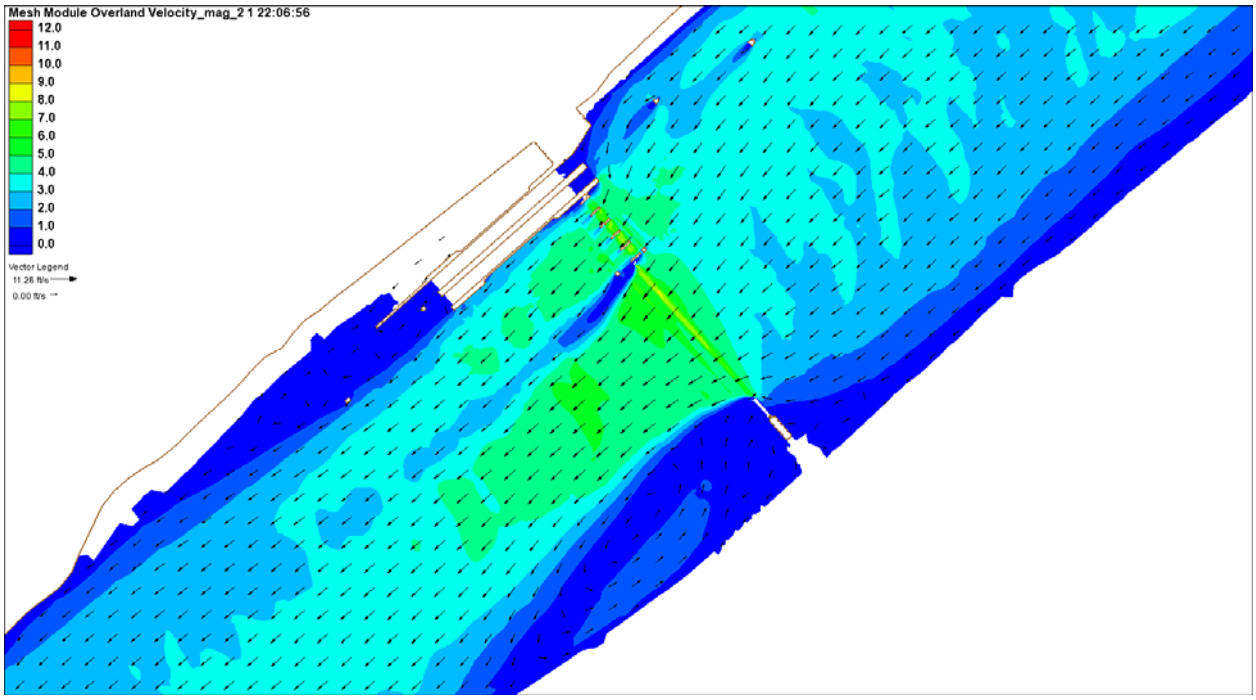

Figure 56. Condition 1 velocities in feet per second.

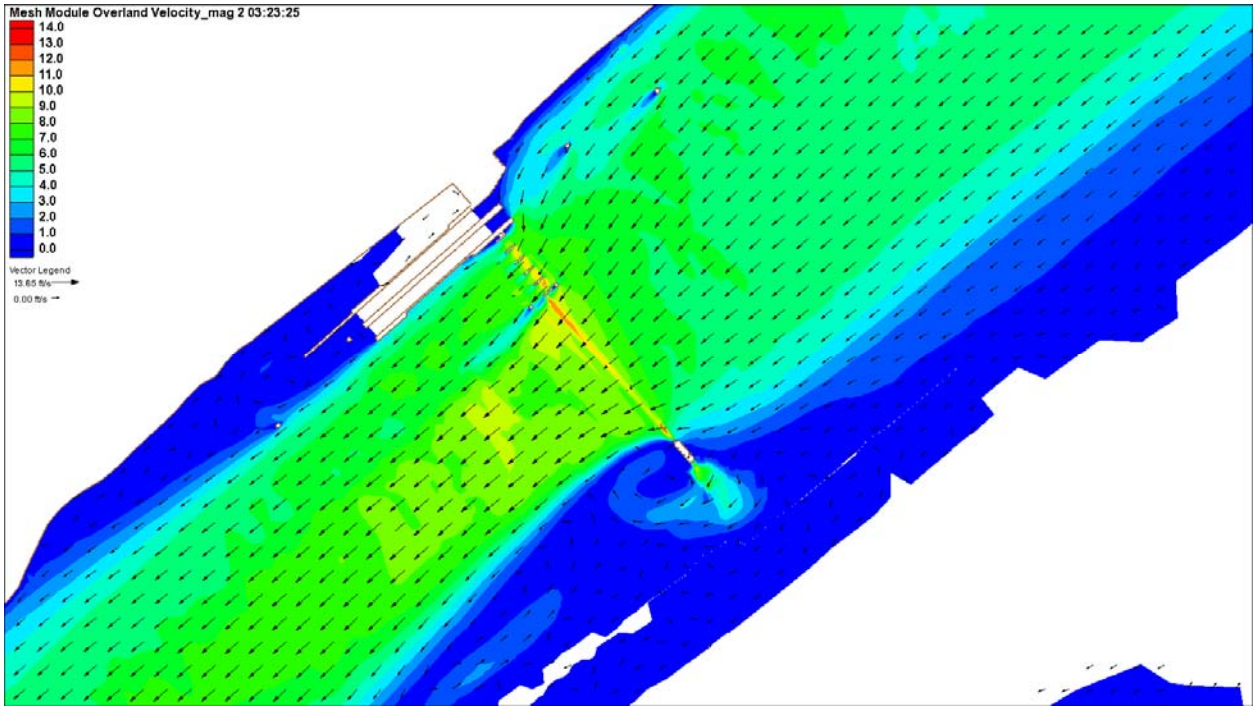

Figure 57. Condition 2 velocities in feet per second.

6 Discussion

This modeling effort has identified two main areas of concern. First is those areas related to the currents and safe navigation of vessels. Second, scour issues might undermine the cofferdam structure causing a structural failure. Both represent serious issues that could have negative impacts to the viability of this new ITD construction alternative.

6.1 Navigation/Currents

For both phases of cofferdams, there are locations in the flow fields that could create adverse navigation conditions.

As expected for the two phases, the velocity peaks occur at the greatest choke point. Peak velocities for the Phase 1 cofferdam occur over the rock dike downstream of the structure, favoring the deflector wall. The maximum velocity for Condition 1 is approximately 10 fps and approximately 15 fps for Condition 2. Peak velocities for Phase 2 occur over the wicket gate dam section and again favor the deflector wall side. Here, the maximum velocity is approximately 14 fps for Condition 1 and 18 fps for Condition 2. The peak velocity locations represent a potential navigation hazard if a vessel is unable to power through the currents. Stalling in the pass would block traffic and require the stalled vessel to carefully reverse direction.

The currents generated in the Phase 2 cofferdam appear to create a greater hazard then those in Phase 1. This is due to four facts: First, the navigable pass section containing the wicket gates is in place for this flow field, creating a higher sill elevation. Second, the navigation pass is 90 ft narrower than Phase 1. Both contribute to a greater choke point for Phase 2. Third, the thalweg of the channel is closer to the right descending bank, forcing a flow split such that the radius of curvature of the flow is greater for Phase 2. This generates a greater super elevation along the left descending bank that creates a larger head differential across the channel, adding to the peak velocity along the deflector wall. Finally, the flow split creates a greater head difference between the upstream and downstream sides of the cofferdam.

For Phase 2 conditions, there are currents that wrap around the Kentucky bank cells forming a cross current. This cross current may be significant

enough to force an up-bound tow's bow to port, requiring corrective maneuvering, furthering the drift of the vessel to port. This maneuver could potentially force the vessel into the cofferdam/deflector wall. Additionally, the vortex shedding that occurs downstream of the cofferdam may also cause adverse navigation conditions.

6.2 Scour issues

Using the bed shear as an indicator for potential scour provides a means to highlight areas subject to sediment motion. For Phase 1, the areas of concern are the upstream tip of the cofferdam guard wall, through the navigation pass where bed shear peaked above the rock dike, and the Kentucky bank tie back. For Phase 2, the areas of concern are the upstream and downstream tips of the cofferdam guard wall and the tie back on the Kentucky bank side. Proper armoring and monitoring will be required in all mentioned locations.

The maximum shear stress in each phase and condition provide an evaluation of the critical shear stress potential. For Phase 2-Condition 2, the maximum scour is 75 Pa and is sufficient enough to initiate movement of a small to large cobble particle (Julien 2002). This represents the largest bed shear stress for the four tests. Phase 1-Condition 2, Phase 2-Condition 1, and Phase 1-Condition 1 have a max bed shear stress of 65, 25, and 14 Pa, respectively. See Table 8 to relate these shear stresses to the mobilization of bed material. All are fully capable of mobilizing the sand bed of the Ohio River.

Table 8. Particle size related to critical shear stress (Julien, 2002).

Class Name	Particle diameter in millimeters	Critical Shear Stress in Pascals
Cobble		
Large	>128	111
Small	>64	53
Gravel		
Very coarse	>32	26
Coarse	>16	12
Medium	>8	5.7
Fine	>4	2.71
Very fine	>2	1.26
Sand		

Class Name	Particle diameter in millimeters	Critical Shear Stress in Pascals
Very coarse	>1	0.47
Coarse	>0.5	0.27
Medium	>0.25	0.194
Fine	>0.125	0.145
Very Fine	>0.062	0.11

7 Recommendations

- With the possibility of significant scour in the area of the navigation passes and cofferdams, it is recommended that the 1:120 scale Olmsted Physical Model at CHL should be implemented with the new cofferdam configurations to evaluate scour potential and magnitude.
- Sediment will likely deposit downstream of the cofferdams due to the formation of slack water and vortices. This will require dredging to remove the shoals for maximum vertical navigation clearances at Olmsted.
- By using the lock chambers to pass flow, debris and sediment may accumulate, which will require cleaning prior to lock operation.
- Scour protection will be needed on the Kentucky bank tie back. This is the section that links the Kentucky bank to the cells and was shown to have some significant overtopping velocities in the high flow event.
- With limited vessel current interaction in AdH, certain potentially hazardous phenomenon were not accounted for, namely tow-bow-diving ("submarining a tow"). A physical model study could be implemented to evaluate this potential at Olmsted.
- Real-time velocity monitoring of the navigation passes is encouraged to provide current data to pilots, such that the pilots can determine the navigability of the passes and assist with determining the need for helper boats.
- ADCP measurements should be made upstream, in, and downstream of the navigation passes while the cofferdams are in place. This will help further validate the AdH 2012 for future efforts.

References

Ahlborn, B., M. L. Seto, and B. R. Noack. 2002. On drag, Strouhal number and vortex-street structure. *Fluid Dynamics Research* (30)379-99.

Berger, R. C., and R. L. Stockstill. 1999. A finite element system for flows. In *Proceedings of the 1999 Water Resource Engineering Conference, Seattle, WA, American Society of Civil Engineers*.

Berger, R. C., and L. Lee. 2005. *Modeling of Vessel Effects: Selection of Adaption Parameters for Modeling Vessels in AdH*. ERDC CHL CHETN-IX-15.

Isakson, A. 1937. On the formula for the velocity distribution near walls. *Journal of Technical Physics (U.S.S.R.)* 155.

Jones, G. W., Jr. 1968. Unsteady lift forces generated by vortex shedding about a large, stationary, oscillating cylinder at high Reynolds Numbers. ASME Symposium Unsteady Flow.

Julien, P. Y. 2002. *River Mechanics*. Cambridge: Cambridge University Press.

Millikan, C. M. 1938. A critical discussion of turbulent flows in channels and circular tubes. In *Proceedings 5th Intl Congress of Applied Mechanics*, 386-392. John Wiley and Sons.

Roshko, A. 1961. Experiments on the flow past a circular cylindar in at very high Reynolds Number. *Journal of Fluid Mechanics*, 10(3):603-12.

Stockstill, R. L., and R. C. Berger. 1999. *Interim report for the Upper Mississippi River-Illinois Waterway System Navigation Study, A two-dimensional flow model for vessel-generated currents*. ENV Report 10. Vicksburg, MS: US Army Engineer Waterways Experiment Station.

Stockstill, R. L., and R. C. Berger. 2001. Simulation of flow in hydraulic structures using AdH. In *Proceedings of the World Water & Environmental Resources Congress, Orlando FL*, May 20-24, 2001.

Wagner, C. R. 2004. Results of a Two-Dimensional Hydrodynamic and Sediment-Transport Model to Predict the Effects of Phased Construction and Operation of the Olmsted Locks and Dam on the Ohio River near Olmsted, Illinois. Water-Resources Investigations Report 03-4336, USGS.

White, F. M. 2003. *Fluid Mechanics: Fifth Edition*. New York: The McGraw-Hill Companies, Inc.

Appendix: Additional Simulations

The additional simulations had a higher tailwater elevation than the above runs. For Condition 1, the tailwater was set at 295 ft, and for Condition 2, it was set at 320 ft. These produced a WSE at Olmsted of approximately 297 and 323 ft, respectively.

	Phase 1 - Condition 1		Phase 1 - Condition 2	
X-Sec	*High Tailwater*	*Low Tailwater*	*High Tailwater*	*Low Tailwater*
964.18	3.54	3.64	6.25	6.84
964.417	5.07	5.28	8.87	9.68
964.459	5.31	5.56	9.30	10.14
964.573	4.95	5.23	8.77	9.58

	Phase 2 - Condition 1		Phase 2 - Condition 2	
X-Sec	*High Tailwater*	*Low Tailwater*	*High Tailwater*	*Low Tailwater*
964.18	3.52	3.82	5.28	5.58
964.417	5.03	5.39	7.89	8.55
964.459	7.36	8.11	10.96	12.04
964.573	5.11	5.38	9.21	9.87

	Phase 1 - Condition 1		Phase 1 - Condition 2	
X-Sec	Low Tailwater	High Tailwater	Low Tailwater	High Tailwater
964.18	295.08	297.69	320.91	323.85
964.417	294.83	297.47	320.01	323.09
964.459	294.72	297.38	319.67	322.80
964.573	294.61	297.30	319.47	322.65
Swell Head	0.47	0.39	1.44	1.20

	Phase 2 - Condition 1		Phase 2 - Condition 1	
X-Sec	Low Tailwater	High Tailwater	Low Tailwater	High Tailwater
964.18	295.39	298.00	321.87	324.57
964.417	295.11	297.76	321.02	323.86
964.459	294.55	297.31	319.96	323.02
964.573	294.47	297.21	319.23	322.44
Swell Head	0.92	0.79	2.64	2.13

REPORT DOCUMENTATION PAGE

Form Approved
OMB No. 0704-0188

1. REPORT DATE *(DD-MM-YYYY)*	2. REPORT TYPE	3. DATES COVERED *(From - To)*
July 2013	Final	

4. TITLE AND SUBTITLE

2D Hydrodynamic Investigation of Olmsted Cofferdams

5a. CONTRACT NUMBER

5b. GRANT NUMBER

5c. PROGRAM ELEMENT NUMBER

6. AUTHOR(S)

Jeremy A. Sharp, Tate. O. McAlpin, Ronald E. Heath, Gary C. Lynch, and Howard E. Park

5d. PROJECT NUMBER

5e. TASK NUMBER

5f. WORK UNIT NUMBER

7. PERFORMING ORGANIZATION NAME(S) AND ADDRESS(ES)

Coastal and Hydraulics Laboratory
US Army Engineer Research and Development Center
3909 Halls Ferry Road
Vicksburg, MS 39180

8. PERFORMING ORGANIZATION REPORT NUMBER

ERDC/CHL TR-13-6

9. SPONSORING / MONITORING AGENCY NAME(S) AND ADDRESS(ES)

US Army Corps of Engineers Louisville District
Romano Mazzoli Federal Building
600 Dr. Martin Luther King, Jr. Place
Louisville, KY 40202

10. SPONSOR/MONITOR'S ACRONYM(S)

11. SPONSOR/MONITOR'S REPORT NUMBER(S)

12. DISTRIBUTION / AVAILABILITY STATEMENT

Approved for public release; distribution is unlimited.

13. SUPPLEMENTARY NOTES

14. ABSTRACT

The Olmsted Locks and Dam are currently being constructed on the Ohio River just downstream of Lock and Dam 53 at river mile 964.4. The original Olmsted construction plan called for an in-the-dry (ITD) construction using a four-phase cofferdam configuration; however, as a cost saving measure, planners changed the original plan to construct the dam using an in-the-wet (ITW) construction process. Cost and schedule concerns with ITW have US Army Corps of Engineers (USACE) leaders investigating all options to minimize overall project cost, time, and navigation impacts. Thus, USACE Louisville District (LRL) has proposed a two-phase cofferdam plan to replace the ITW construction. To evaluate the effect of the newly proposed cofferdam configurations an Adaptive Hydraulics Model (AdH) was developed to provide current velocities and depths for the Ship Tow Simulator (STS) for pilots to evaluate the navigability of the proposed cofferdam configurations. In addition, the AdH model was used to evaluate areas of scour around the cofferdams qualitatively. Two stages and discharges were simulated. A maximum velocity through the navigation passes are from 10 – 18 feet per second (fps), and bed shear stresses are estimated at 14 -75 Pascals (PA). Both could negatively affect the viability of this two-phase cofferdam construction alternative.

15. SUBJECT TERMS

Control structure
Hydrodynamics
Lock and dam
Navigation
River
Ship simulator
Steady state
Vortex

16. SECURITY CLASSIFICATION OF:			17. LIMITATION OF ABSTRACT	18. NUMBER OF PAGES	19a. NAME OF RESPONSIBLE PERSON: Jeremy A. Sharp
a. REPORT	b. ABSTRACT	c. THIS PAGE			19b. TELEPHONE NUMBER *(include area code)*
Unclassified	Unclassified	Unclassified	Unclassified	62	601-634-4212